Title

Interspecies Comparisons of Xenopus Egg Extracts Reveal Mechanisms for Modulating Meiotic Spindle Size and Architecture

Author

Helmke, Kara

Publication Date

2014

Peer reviewed|Thesis/dissertation

Interspecies Comparisons of *Xenopus* Egg Extracts Reveal Mechanisms for Modulating Meiotic Spindle Size and Architecture

By

Kara J Helmke

A dissertation submitted in partial satisfaction of the

requirements for the degree of

Doctor of Philosophy

in

Molecular and Cell Biology

in the

Graduate Division

of the

University of California, Berkeley

Committee in charge:

Professor Rebecca Heald, Chair
Professor Karsten Weis
Professor Georjana Barnes
Professor Mohammad Mofrad

Spring 2014

Interspecies Comparisons of *Xenopus* Egg Extracts Reveal Mechanisms for Modulating Meiotic Spindle Size and Architecture

Abstract

Interspecies Comparisons of *Xenopus* Egg Extracts Reveal Mechanisms for Modulating Meiotic Spindle Size and Architecture

By

Kara J Helmke

Doctor of Philosophy in Molecular and Cell Biology

University of California, Berkeley

Professor Rebecca Heald, Chair

The function of the spindle to faithfully segregate chromosomes is universal among eukaryotes. A common feature of metaphase spindles is their self-organizing, bipolar structure, with microtubules organized into polar arrays by the activity of motors and other proteins. However, wide variation in spindle assembly, size and morphology is observed among different cell types, presumably to optimize spindle function. While many of the hundreds of conserved spindle assembly factors have been identified, how these proteins interact to establish a particular spindle architecture is poorly understood.

Xenopus provides a valuable system to study a variety of spindle types *in vitro*, since spindles formed in egg and embryo extracts recapitulate morphologies observed *in vivo*. The ellipsoidal, ~35 μm long *Xenopus laevis* meiotic spindle has been studied most extensively and is thought to be built from a tiled array of dynamic, overlapping microtubules. Meiotic spindles assembled in egg extracts of the smaller *Xenopus tropicalis* frog possess a similar anastral appearance but are significantly shorter at ~22 μm. Previously, these two extracts were used to identify proteins which regulate spindle length, and a microtubule-severing protein p60 katanin was shown to be differentially phospho-regulated between these two systems. However, activity differences in p60 katanin were not sufficient to explain the size differences between *X. tropicalis* and *X. laevis*, and this study identifies TPX2 as an additional length regulator that also contributes to other features of spindle architecture.

In addition to evaluating spindle length, we probed the involvement of microtubule nucleation, motor-dependent organization, and microtubule distribution as contributors to architectural features. Spindles formed in *X. laevis* extracts have been previously shown to rely heavily on both microtubule nucleation near chromatin governed by the protein RanGTP as well as organization of antiparallel arrays by the kinesin-5 motor Eg5, resulting in a structure with a tiled array of microtubules with nearly uniform density pole-to-pole. Intriguingly, *X. tropicalis* extract spindles do not require either process, as indicated by resistance to inhibition of these pathways. Furthermore, *X. tropicalis* microtubule density is significantly reduced in the spindle midzone.

We focused on the role of the microtubule-associated factor TPX2 in mediating these differences, since it has been shown to interact with both Ran and Eg5. Levels of TPX2 were measured to be approximately 3-fold higher in *X. tropicalis*. Addition of excess TPX2 to *X. laevis* extract recapitulated differences seen in the architectures of the two spindles: rendering them less sensitive to RanGTP and Eg5 inhibition as well as reducing spindle length. These spindles also showed increased recruitment of Eg5 to the spindle poles, where microtubule density increased. We propose that TPX2 levels modulate spindle architecture by partitioning microtubules between a tiled antiparallel array that promotes spindle expansion, and a compact, parallel cross-linked architecture that concentrates MTs at spindle poles.

Additionally, TPX2 has been previously shown in the literature to have microtubule-nucleating activity. Examining the two *Xenopus* species orthologs of this protein, we determined that *X. tropicalis* had much higher nucleation capacity, resulting in spindle astral microtubules not normally seen in the *Xenopus* egg extract spindle as well as increased non-spindle associated microtubule formation. Comparing primary sequence of these proteins, we discovered a short c-terminal 7 amino acid sequence absent from the *X. tropicalis* protein. Removing this sequence from *X. laevis* TPX2 greatly enhanced microtubule nucleation and altered spindle morphology. Using these TPX2 nucleation mutants in spindle assembly, we were able to ask what the effect of altering microtubule nucleation was on spindle length. Surprisingly, changing microtubule nucleation did not affect spindle length but did determine the presence of astral microtubules at spindle poles.

In summary, we show here how TPX2 is involved in many features of spindle architecture: establishing MT distribution and spindle length through its interaction with Eg5, and polar architecture through its nucleation activity. TPX2 is not well-conserved through evolution, and many species retain only certain protein domains of the protein, and therefore only a subset its activities. As a major contributor to spindle architecture, it is an attractive hypothesis that species tailor their spindle morphology through evolutionary retention or rejection of certain TPX2-mediated architectural features.

TABLE OF CONTENTS

LIST OF FIGURES

ABBREVIATIONS

APC/C Anaphase Promoting Complex/Cyclosome
Ca2+ calcium
CPC Chromosomal Passenger Complex
CSF Cytostatic Factor
Da Dalton
EB1 End-binding protein 1
FRET Fluorescence Resonance Energy Transfer
GDP Guanosine Diphosphate
GFP Green Fluorescent Protein
GTP Guanosine Triphosphate
IC_{50} half-maximal inhibitory concentration
kin kinesin
k-MT kinetochore MT
k-fiber kinetochore fiber
MAP microtubule associate protein
MCAK Mitotic Centromere Associated Kinesin
MT microtubule
MTOC microtubule organizing center
Ncd Non-claret disjunctional protein
NuMA Nuclear Mitotic Apparatus
Op18 Oncoprotein 18
Plx1 Polo-like kinase in Xenopus 1
PCM pericentriolar material
RCC1 Regulator of Chromosome Condensation
SAF spindle assembly factor
ssp1 short spindle phenotype 1
TPX2 Targeting Protein for Xklp2
γ-TuRC Gamma-Tubulin Ring Complex
Xklp2 *Xenopus* kinesin-like protein 2
X. tropicalis Xenopus tropicalis
X. laevis Xenopus laevis

ACKNOWLEDGEMENTS

I am indebted to many people for their help and encouragement in completing this work. Firstly, and perhaps most importantly, is my advisor, Rebecca Heald, who I think accepted me into her lab based solely on my enthusiasm and less on my scientific prowess. Her guidance was always available (and always positive), but I appreciate the freedom she gave me to find my own way and to learn to think independently, and for knowing when that was tough and handing me a margarita.

My other advisors are many. My thesis committee, Georjana Barnes, Mohammad Mofrad, and Karsten Weis, who gave me unquestionable support throughout my research but also during tenuous times when I was deciding on my next step. I want to additionally thank Karsten for being a second mentor to me. Despite me not choosing his lab to do my thesis work, I DID choose a lab where I could still call upon him as a mentor, and he truly is exceptional in that regard. I had the privilege to teach with him and learn from him, and he helped cultivate my passion for education.

This project would have gone nowhere without two important lab members: Rose Loughlin and Jeremy Wilbur. They, surprisingly, let me spout my ignorance at them on a regular basis and then gently or bluntly, respectively, mentored me into good science. I have learned more about science, and how to do science, from these two people than any other source on the planet. And I also learned never to study katanin.

The Heald lab has been home to many amazing and interesting people over the years, among them Beno Freedman, Blake Riggs, David Halpin, Dan Levy, Anne-Lore Schlaitz, Kieren Patel, Steve Bird, Kelly Miller, Esther Kieserman, Magdalena Strzelecka, Yasaswini Sampathkumar, Matthew Good, Marina Ellefson-Crowder, Andy Lane, Andrew Grenfell, Romain Gibeaux, and Chris Brownlee. Everyone contributed to my graduate work in some way, and I am so grateful for having known and worked with each of them. Without naming each person, I want to acknowledge the entire Trilab and how amazing it's been to feel part of a bigger community than just one lab. Let's hope the new incarnation of the Trilab carries on that tradition!

Of course, my appreciation for my family for their love and support cannot go unsaid. I thank them for bearing with me and letting me move across the country to spend years in school. Special thanks to my sister (/best friend) for giving me an amazing niece and godchild, who is an excellent excuse to come visit, not that I needed one.

Last, and *certainly* not least, I thank my husband Charlie for being there every single day. For countless chauffeured trips to and from the lab at all hours of the day, for not resenting all the weekends spent running last experiments, for dealing with me when the lows of science became very low and celebrating when the highs became very high. When I got offered an amazing job opportunity, knowing that it would take a year of working two jobs and 18-hour days, his first and immediate response was, "Let's do it." I can't thank him enough, but will try to do so by actually seeing him more these days.

Chapter 1: Introduction

The spindle is a complex, self-assembling, and dynamic structure that performs the crucial task of chromosome segregation during cell division. At steady state, the spindle is constantly turning over its component microtubules (MTs), which are regulated by hundreds of associated proteins. While many universal and conserved principles operate to ensure proper chromosome segregation, we seek to elucidate the mechanisms that result in elaboration of certain spindle features.

I. Spindle Components and Assembly[1]

Dynamic MTs are the Fundamental Structural Unit of the Spindle

MTs are polymers made of α- and β-tubulin heterodimers that bind head-to-tail to form polarized protofilaments, and in turn ~13 protofilaments associate laterally and in the same orientation to form a hollow rigid tube about 25 nm in diameter (Chrétien et al., 1992; Downing and Nogales, 1998). The asymmetry of the tubulin dimer confers polarity to the polymer – the end with exposed α-tubulin is called the minus-end, while the β-tubulin end is the plus-end – leading to different polymerization and depolymerization reactions at each end.

MTs may be growing or shrinking, and can abruptly switch between the two states, a behavior termed dynamic instability (Mitchison and Kirschner, 1984a; 1984b). Following polymerization, hydrolysis of GTP bound to β-tubulin occurs rapidly within the lattice of the MT, and MTs possessing a terminal "cap" of tubulin dimers that have not yet hydrolyzed their GTP can maintain the growing state. If the terminal tubulin dimers hydrolyze their β-tubulin GTP, the MT loses its cap and switches to a depolymerizing state, a transition called "catastrophe". Conversely, a shrinking MT that regains its GTP tubulin cap can resume growing, a so-called "rescue" (Figure 1.1). The dynamics of MTs can be further regulated by motors or associated proteins, which promote or inhibit these transition states.

[1] Content for Chapter 1:Section I contains excerpts and figures from the author's previously published work (Helmke et al., 2013).

Figure 1.1

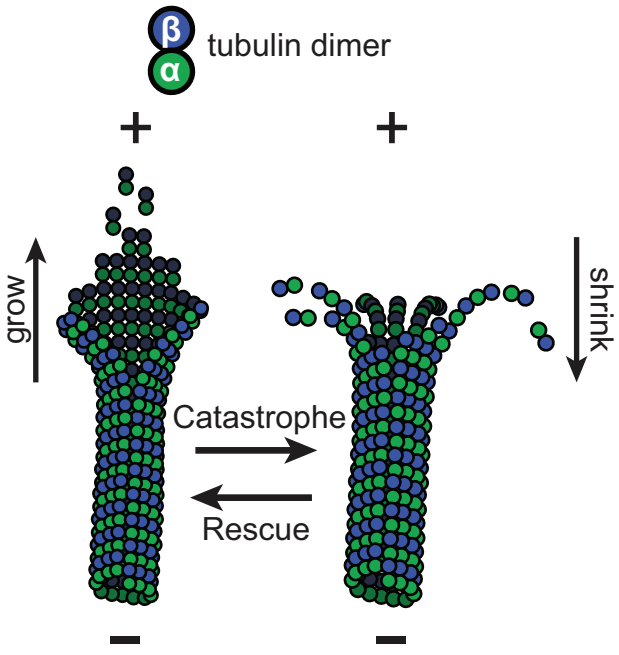

Figure 1.1 MT structure and dynamics
A MT is a hollow cylindrical structure built from ~13 parallel protofilaments of α/ β-tubulin heterodimers. The subunits in each protofilament all point in the same direction, giving the MT lattice a distinct structural polarity, with α-tubulin exposed at the minus-end and β-tubulin exposed at the plus-end. Following polymerization, GTP hydrolysis within β-tubulin destabilizes the MT, but if the polymerization rate is sufficiently high, a GTP cap is maintained and the MT continues to grow. If hydrolysis catches up to the end, the GTP cap is lost, and the MT undergoes a catastrophe and shrinks as its protofilaments peel apart. If the GTP cap is regained, a rescue occurs and MT growth resumes. Adapted from (Helmke et al., 2013).

Spindle Assembly Pathways Rely on Positional Nucleation of MTs

There are two recognized spindle assembly pathways, “search-and-capture” and “spindle self-organization”, which are not mutually exclusive and are thought to operate simultaneously in most cases to promote robust spindle formation. These two pathways are broadly defined by where MTs nucleate. Search-and-capture occurs by selective stabilization of MTs nucleated at the MT organizing center (MTOC) or centrosome, and self-organization describes any number of modes of nucleation followed by incorporation of the MTs into a bipolar array by the activity of associated proteins including MT-based motors. Less well understood, however, is what determines the relative role of a pathway or the preferred types of MT nucleation in a particular cell type, and how these pathways are inter-regulated and contribute to spindle architecture. Depending on where and how MTs are nucleated, the proportion of MTs in each population may change, thereby altering organization of the spindle.

Centrosome-mediated search-and-capture

Since MT dynamic instability was first observed, Mitchison and Kirschner proposed that spindle assembly could occur through the selective stabilization of centrosome-nucleated MTs at kinetochores (Mitchison and Kirschner, 1985). By frequently switching between growing and shrinking states, MTs can “probe” the cytoplasm randomly until captured by a chromosome, allowing the cell to gradually form a bipolar MT array from two centrosomes and pairs of sister chromatids (Figure 1.2A; Holy and Leibler, 1994). When present, centrosomes appear to be the dominant MT generating and organizing centers of the cell. A typical centrosome consists of a pair of centrioles surrounded by pericentriolar material (PCM) that recruits the tubulin isoform γ-tubulin in a complex called the γ-tubulin ring complex (γ-TuRC) that provides a template for MT growth by stabilizing and anchoring the minus-ends of MTs at the centrosome (Hannak *et al.*, 2002; Kollman *et al.*, 2010; Guillet *et al.*, 2011; Kollman *et al.*, 2011).

While a simple and appealing model, computational simulations indicated that search-and-capture would be rather inefficient on its own and require hours longer than the time period of a normal mitosis (Wollman et al., 2005). However, the time could be reduced if geometric constraints were added to the model that optimized the size and spatial exposure of target kinetochore binding sites to centrosome-nucleated MTs, specifically by increasing chromosome mobility and by incorporating chromosome-dependent MT nucleating pathways discussed below (Paul et al., 2009). Despite the prevalence of centrosomes, the existence of meiotic or plant spindles that lack them, together with studies employing centrosome ablation, clearly demonstrate that they are not essential for bipolar spindle assembly (Khodjakov et al., 2000).

In addition to promoting bipolarity, centrosomes and associated factors can regulate spindle length. In the *C. elegans* embryo, spindle size correlates with centrosome size, and molecular perturbations that altered centrosome size proportionally changed spindle length (Greenan et al., 2010). How centrosome size is established is not understood, but a spindle associated TPX2-like protein (discussed below) in *C. elegans* has been implicated and might provide a molecular link between the centrosome and spindle architecture.

Figure 1.2

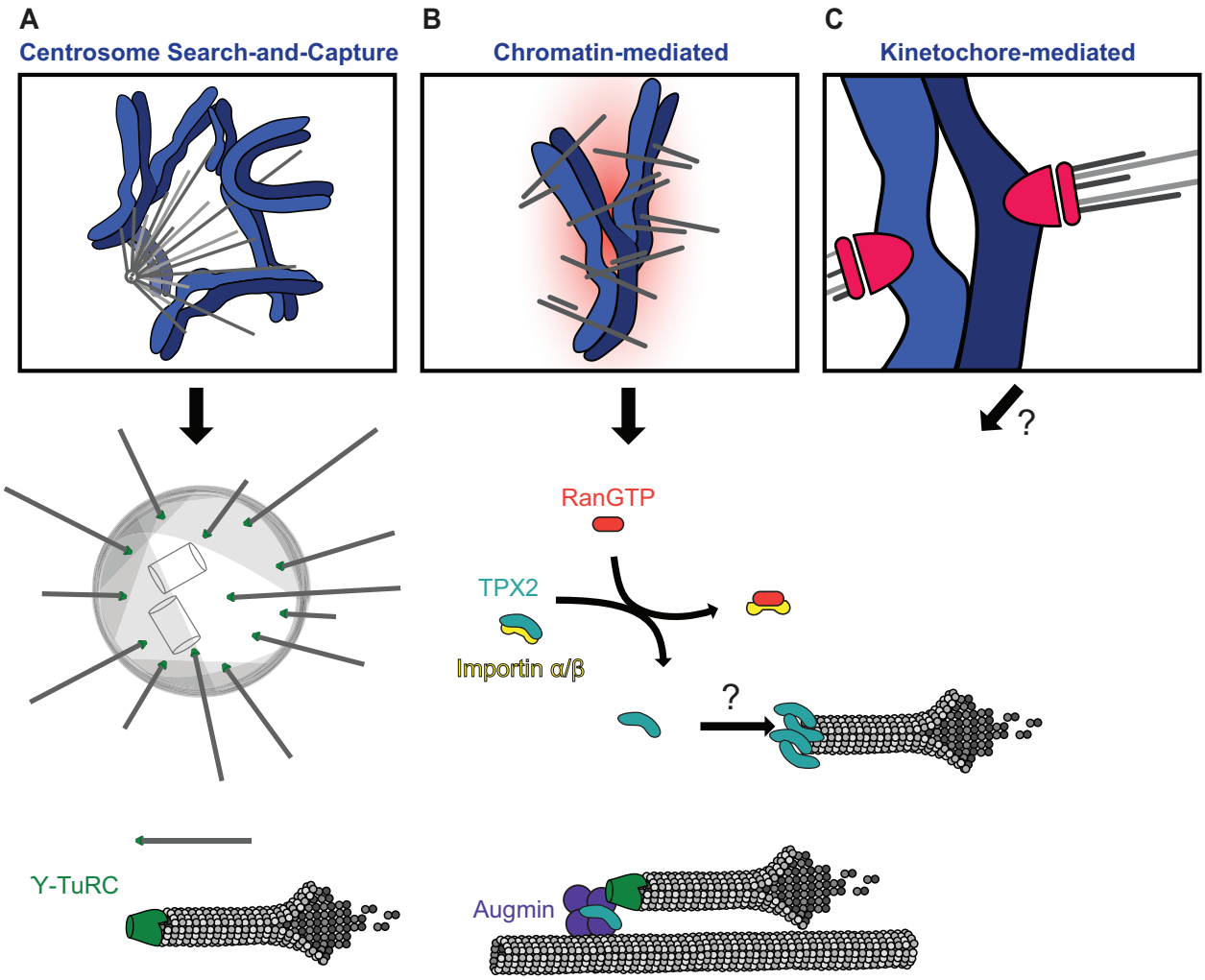

Figure 1.2 Spindle assembly pathways and mechanisms of MT nucleation
(A) Centrosome-mediated search-and-capture proceeds by nucleation of MTs from the γ-tubulin ring complex embedded in the centrosome. Orientation of chromosomes in a toroidal arrangement around the center of the nascent spindle, with exposed kinetochores, facilitates connections between these centrosomal MTs and kinetochores.

(B) The chromatin-mediated self-assembly pathway is governed by a spatial gradient of RanGTP, which stimulates release of MAPs in the vicinity of the chromosomes. One confirmed cargo, TPX2, has a role in nucleation of MTs in this pathway, but the mechanism is unknown. The Augmin complex, which recruits γ-TuRC, amplifies MTs nucleated around the chromosomes in this pathway.

(C) MTs have been shown to nucleate directly from kinetochores, however, the mechanism is not yet elucidated, but might share some commonalities with the chromatin-mediated pathway. Adapted from (Helmke et al., 2013)

Mitotic chromatin-mediated nucleation

Experiments using *Xenopus* egg extracts demonstrated that MTs nucleated around chromatin-coated beads could organize into a bipolar spindle structure in the absence of both centrosomes and kinetochores, illustrating the self-organization pathway of spindle assembly (Heald et al., 1996). In both egg extracts and human tissue culture cells, chromatin effects are mediated primarily by a gradient of GTP-bound Ran, which peaks at the chromosomes. Single glass beads coated with RCC1, the guanine nucleotide exchange factor that loads Ran with GTP, could induce bipolar spindle assembly in *Xenopus* egg extracts, indicating that generation of RanGTP is sufficient for spindle formation (Halpin et al., 2011). However, RCC1 bead spindles were unstable and displayed abnormal MT density, indicating that other chromatin factors are required to generate an architecturally normal spindle. The RanGTP gradient induces spindle formation by triggering the release of spindle assembly factors (SAFs) from inhibitory interactions with the transport molecules importin α/β, resulting in MT nucleation and organization around mitotic chromatin. Motor proteins organize the MTs into an antiparallel array by sliding them away from the chromatin and focusing their minus-ends into spindle poles. In cell types with centrosomes, clustering of MT minus-ends may also be facilitated by enriching of MT binding or motor proteins at the centrosomes or by the astral MTs, which provide tracks on which to focus the antiparallel array (Compton, 1998). How MTs are nucleated downstream of RanGTP is not yet clear, though one proposed candidate is TPX2 (discussed below).

In addition to activating spindle assembly factors (SAFs) by liberation from importins, new evidence has revealed a role for Ran in regulating the Anaphase Promoting Complex/Cyclosome (APC/C)-induced degradation of certain SAFs during mitosis and spindle assembly. The APC/C has been localized to the spindle poles, and its inhibition resulted in aberrant spindle phenotypes, suggesting a role for the APC/C in spindle maintenance before the spindle checkpoint is satisfied and prior to anaphase (Tugendreich *et al.*, 1995; Kraft *et al.*, 2003; Ban *et al.*, 2007; Goshima *et al.*, 2007; Somma *et al.*, 2008; Williamson *et al.*, 2009). One model is that an additional layer of spatial and temporal regulation on Ran cargoes is generated: RanGTP liberates them from importin β to perform their assembly and MT stabilizing tasks, but limits their lifetime in the spindle by rendering them susceptible to ubiquitylation by the APC/C (Song and Rape, 2010). This subtle mode of regulation implies that Ran-regulated SAFs are powerful modulators of spindle architecture that require precise temporal and spatial regulation to generate a functional spindle.

In addition to the factors regulated by Ran/importin binding, the chromatin-mediated pathway includes additional signals generated by the chromosome passenger complex (CPC) (Ruchaud et al., 2007). In most organisms, the CPC consists of the mitotic kinase Aurora B and associated factors that regulate its activity and targeting: INCENP, Survivin, and Borealin/Dasra. CPC activity is essential in some cases of acentrosomal spindle assembly, such as in *Drosophila* meiosis and in *Xenopus* egg extracts (Sampath *et al.*, 2004; Gadea and Ruderman, 2005; Colombié *et al.*, 2008). The contribution of the CPC to chromatin-mediated spindle assembly is primarily through Aurora B-dependent phosphorylation and inhibition of MT destabilizing proteins

Op18/Stathmin and the kinesin-13 MCAK, thereby promoting MT stability in the vicinity of chromosomes (Ohi *et al.*, 2004; Gadea and Ruderman, 2006).

Kinetochore-driven nucleation

Early studies from Brinkley and McIntosh described MTs polymerizing from kinetochores, but until more recently this was not demonstrated in live cells (Figure 1.2C) (Pepper and Brinkley, 1979; Khodjakov, 2003; Maiato, 2004). While the molecular mechanism of MT nucleation at the kinetochore is unknown, there is evidence that this process, like chromatin-mediated spindle assembly, requires the small GTPase Ran (Tulu *et al.*, 2006; Torosantucci *et al.*, 2008). Whatever the mechanism for kinetochore-mediated nucleation of MTs, it is clear that establishing close contact of MTs with kinetochores early during spindle assembly likely improves the kinetics of assembly by increasing the effective size of the kinetochore target during search-and-capture. Furthermore, kinetochore-mediated nucleation may contribute directly to k-fiber formation.

MT-branching nucleation

The idea of existing MTs acting as templates for new MT nucleation and growth stems from observations in *Drosophila* S2 cells and *Xenopus* extracts showing that MT plus-ends, as visualized by fluorescently labeled EB1, appear throughout the body of the spindle, indicating nucleation at points distinct from centrosomes or chromosomes (Tirnauer *et al.*, 2004; Mahoney *et al.*, 2006). Furthermore, plant cortical arrays clearly generate branched MT arrays, though the underlying molecular mechanism remains unknown. In animals, this MT nucleating activity is mediated by an 8-member complex called Augmin originally identified in *Drosophila*, and its depletion resulted in severe loss of spindle MTs (Goshima et al., 2008; Uehara et al., 2009). An interaction between the Augmin complex and γ-TURC was shown to be essential for its MT nucleation in human cells, and a similar interaction is predicted for *Drosophila* (Uehara et al., 2009). This suggests a model in which Augmin binds to preexisting MTs and recruits γ-TURC to nucleate a new MT (Figure 1.2B).

The nucleation of MTs by Augmin could function to promote spindle assembly in two ways. First, nucleation of MTs off of preexisting MTs could quickly bolster MT mass and increase the kinetics of spindle formation, which has experimental support in *Xenopus* egg extracts (Petry et al., 2011). Second, MT-branching nucleation could assist in establishing bipolarity by generating antiparallel overlap through nucleation of MTs along the same axis as the existing spindle array, since polarity of newly branched MTs is maintained (Petry et al., 2013). Further cross-linking of these MTS would then provide structural stability to the spindle.

MT-branching nucleation has interesting implications for spindle architecture. Due to the low angle of branching and the maintenance of MT polarity, nucleation occurring anywhere along an existing MT would likely produce a structure akin to a tiled-array, held together by cross-linking factors and molecular motors. In *Xenopus* egg extracts that form spindles with tiled-array architecture self-organized around chromatin-beads, Augmin depletion defects were severe and resulted in abnormally long, multipolar

spindles (Petry et al., 2011). In contrast, the major mitotic phenotype seen upon Augmin depletion in *Drosophila* were defects in the establishment of the anaphase MT arrays, suggesting branching MT nucleation is most important when antiparallel arrays of MTs are prominent (Uehara et al., 2009). Consistent with this idea, Augmin was found to be dispensable for bipolar spindle in human cells whose spindles normally form in a centrosome-driven pathway, and the presence of centrosomes in *Xenopus* spindles largely mitigated the effects of Augmin depletion (Petry et al., 2011). Together, these data imply that unique spindle architectures are likely established through different modes of MT nucleation and organization, although we do not yet understand how branching MT nucleation sites are positioned and regulated.

MTs are Organized by Motor Proteins

The major plus-end directed motor in the spindle is the kinesin-5 member Eg5/BimC/Kinesin Spindle Protein. Eg5 is a homotetramer capable of binding and cross-linking two MTs (Cole et al., 1994). For antiparallel MTs, which Eg5 seems to preferentially bind, the motor functions to slide both MTs with their minus-ends outward away from the center of the spindle (Figure 1.3A). This establishes a basic plus-end in, minus-end out organization of MTs as well as aligning and cross-linking them in an orientation along the same axis. Disruption of Eg5 by the small molecule inhibitor monastrol results in collapse of the spindle into a monopole structure in *Xenopus* egg extracts (Kapoor et al., 2000). In mammalian cells, Eg5 is required to establish bipolarity of the spindle but not to maintain it (Kollu et al., 2009), since the kinesin-12 HKlp2 provides a redundant function (Vanneste et al., 2009). Additionally, Eg5 sliding of MTs outward is thought to contribute to continuous transport of MTs towards the poles, a property of spindles known as poleward MT flux. Inhibition of Eg5 eliminates flux in *Xenopus* egg extract spindles, but does not drastically change the flux rate in mammalian cells (Miyamoto et al., 2004; Cameron et al., 2006). This difference may reflect alternative spindle architectures in which the extent of the anti-parallel MT overlap in *Xenopus* is much higher. Clearly, Eg5 and its orthologs play a critical role in establishing the antiparallel array of spindle MTs and the spindle architectural features and functions associated with it.

The dominant minus–end directed motors in the spindle are dynein and kinesin-14 class members (including Ncd, HSET, XCTK2). Minus-end directed movement between two antiparallel MTs functions to oppose the MT motion of kinesin-5s. However, one MT could also act as cargo, transported toward the minus-end of another MT, thereby clustering the minus-ends of MTs together. These motors therefore play a critical role in focusing MTs into a coalesced pole. *Drosophila* cells containing disruptions in Ncd, a kinesin-14, display defects in spindle pole integrity (Endow et al., 1994), and pole formation is completely abrogated upon dynein inhibition in the centrosome-independent, self-organizing pathway of spindle assembly around DNA-coated beads in *Xenopus* egg extracts (Heald et al., 1996).

In addition to its role in MT organization, dynein also retains its capacity to carry cargoes toward MT minus-ends and the spindle poles, spatially localizing certain activities. Some dynein cargos are thought to help form and maintain the spindle pole, such as NuMA, which stabilizes the pole structure through assembly of multiple MT binding domains upon formation of higher order oligomers (Figure 1.3B) (Merdes et al., 2000). Dynein also carries a number of motors to the pole, like Eg5 and Xklp2, the outcome of which could alter motor activity depending on local MT organization. For example, Eg5 or other motors that typically slide against antiparallel MTs will encounter a much higher density of parallel MTs at the poles, where it may act instead as a cross-linker (Wittmann *et al.*, 1998; Uteng *et al.*, 2008). By promoting dynamic transport of factors throughout the spindle, motors provide an additional layer of regulation of spindle assembly and maintenance factors.

Figure 1.3

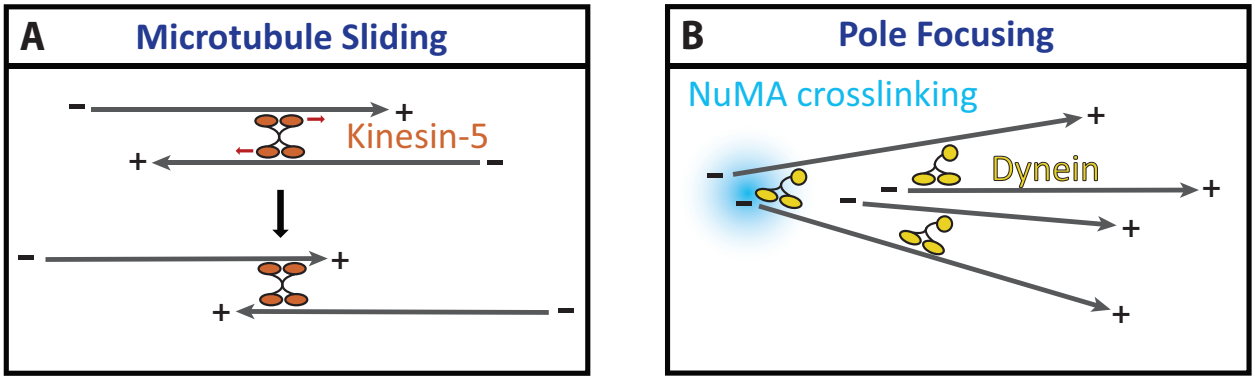

Figure 1.4 Motor Activities in Spindle Organization
(A) In the antiparallel overlap zone, the tetrameric kinesin-5 motor walks to the plus-ends of neighboring MTs, effectively sliding the minus-ends poleward.

(B) Pole focusing occurs through the concerted effort of minus-end directed motors, such as dynein, which carry MTs as cargo towards minus-ends. Additionally, cross-linking activity by NuMA is directed to the poles by dynein transport, where large oligomers cluster MTs.
Adapted from (Helmke et al., 2013)

MT Populations Within the Spindle

Three different populations of MTs define the most basic features of metaphase spindle architecture. The most crucial population is termed kinetochore- or k-fibers (Figure 1.4). K-fiber MTs connect to duplicated chromosomes so that one copy (called a sister chromatid) is attached to each pole of the spindle. The connection occurs at the kinetochore, a macromolecular MT attachment site formed during mitosis at the centromere of each sister chromatid (Jensen, 1982; Rieder, 2005). An interesting property of k-fiber MTs is that they are resistant to treatments that depolymerize other spindle MTs such as cold temperature or low doses of MT depolymerizing drugs. The extensive bundling of k-fibers by MT cross-linking proteins likely increases the stability of their component MTs. The functional effect of k-fiber MT stability may be to provide a rigid connection to chromosomes so that forces are transmitted efficiently and not lost on bending or splaying of k-fiber MTs.

A second population of MTs within the spindle constitutes those that are not part of a k-fiber, referred to here as spindle MTs (Figure 1.4). These MTs may be short and reside within a single half of the spindle or long enough to cross over the center of the spindle to interact with oppositely oriented MTs in an antiparallel fashion (termed interpolar MTs). Spindle MTs are less stable than k-fiber MTs and may be more or less numerous. They appear to increase the rigidity of the spindle to resist to pole-to-pole compression, and may provide a pool of MTs to help maintain k-fibers. However, the role of spindle MTs has infrequently been studied explicitly. In one case, fission yeast spindle MTs extending from each pole were shown to be dispensable for meiotic spindle function (Akera et al.); however, in other systems spindle MTs have a more pronounced role. Depletion of spindle MTs from *Xenopus* egg extract spindles by addition of a tubulin-sequestering protein revealed a role for spindle MTs in establishing proper MT dynamics within the k-fiber, as well as for maintaining spindle size (Houghtaling et al., 2009). In general, larger spindles appear to contain a higher proportion of spindle MTs compared to k-fibers, indicating that they primarily play a structural role.

In addition to the k-fiber and spindle MTs that make up the body of the spindle, a population of astral MTs projects outward toward the cell cortex from the MTOC or centrosome at or near the spindle poles (Figure 1.4). Astral MTs appear less tightly bundled than MTs of the spindle body and, though found in most spindles, they appear to be absent from female meiotic spindles and plant spindles that lack centrosomes. Astral MTs may span the distance from the spindle pole to the cortex and thus provide the cues and forces to properly orient and position the metaphase spindle, which is required for asymmetric cell divisions important for cell fate determination, tissue organization and development (Noatynska et al., 2012).

Figure 1.4

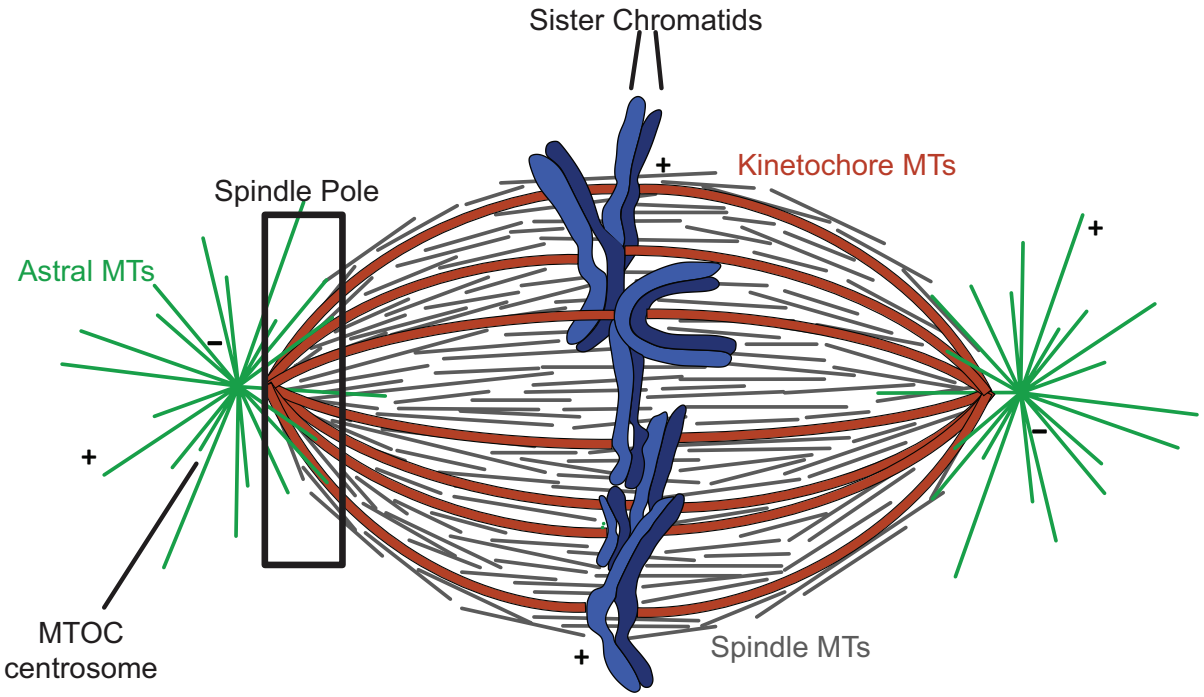

Figure 1.4 Metaphase spindle anatomy and constituent MT populations
MTs are arranged in an antiparallel array with their plus-ends oriented toward the center of the spindle and their minus-ends towards the poles. MTs that connect to the chromosomes at their kinetochores are called kinetochore-fibers or k-fibers (red), and may consist of a single MT or a bundles of MTs depending on the cell type. At metaphase, the sister chromatids of each duplicated chromosome are attached to opposite spindle poles. Spindle MTs (grey) can be long, extending from the pole across the middle of the spindle, or short, forming a tiled array. Astral MTs (green) emanate from the poles or associated centrosomes with their plus-ends extending outward where they may interact with the cell cortex. Adapted from (Helmke et al., 2013)

II. *Xenopus* Egg Extracts as a Model System

Xenopus egg extracts provide a cell-free system that recapitulates many cell cycle events *in vitro*, and thus has been used to investigate spindle assembly and chromosome condensation (Walczak and Heald, 2008). Because of the lack of cell boundaries, this system allows for many experimental perturbations such as protein addition, immunodepletion, and inhibition as well as physical treatments. This ease of manipulation, in comparison to other systems, allows for direct biochemical testing of spindle-associated activities.

The extract, which consists of undiluted cytoplasm, is prepared by centrifugation of *Xenopus* eggs that are naturally arrested in metaphase of meiosis II. Cell cycle arrest is maintained by cytostatic factor (CSF), but extracts can be induced to proceed through mitosis and into interphase for several "cycles" (Wu and Kornbluth, 2008). For spindle assembly to occur, demembranated *Xenopus* sperm nuclei are added to the extract. MT nucleation is induced around the haploid chromosomes which coalesce into a single pole after approximately 15 minutes. With further incubation, additional MTs nucleate to promote bipolar spindle formation, or half-spindles fuse into a single bipolar structure. If the extract is "cycled" into interphase through the addition of calcium, G/S phase processes such as DNA replication and centrosome and kinetochore duplication occur. The interphase extract is induced to return to mitosis with the addition of fresh CSF extract, and spindles form around the newly replicated DNA. These "cycled" spindles therefore contain duplicated chromosomes with robust kinetochore formation and the presence of pole-associated centrosomes (Maresca and Heald, 2006).

While traditional studies were carried out using *X. laevis*, a study in 2007 showed that similar techniques could be applied to the related species *X. tropicalis*. Interestingly, however, spindles formed *in vitro* in *X. tropicalis* were much smaller than their predecessors, ~22 μm compared to ~35 μm in *X. laevis.* Furthermore, when mixed these extracts produce spindles of intermediate length, suggesting compatible cytoplasmic factors played a role in spindle length determination (Brown et al., 2007). An additional study went on to show that spindle length differences were partially explained by differential phospho-regulation of the MT-severing protein p60 katanin. In the small, *X. tropicalis* spindles, katanin contains a serine to alanine mutation that prevents inhibitory phosphorylation, thus rendering the protein more active and MT severing activity higher. Interestingly, the same study determined that *X. tropicalis* k-fibers had higher relative stability and required increased katanin activity for regulation (Loughlin et al., 2011).

Because of the differences noted in architecture – specifically, spindle length and k-fiber stability – and the compatibility of these species' proteins, comparing *X. laevis* and *X. tropicalis* provides an ideal system to probe molecular mechanisms regulating spindle architecture. This work details how the interspecies *Xenpous* system allowed for the identification of TPX2, discussed in the next section, as a regulator of many facets of spindle architecture.

III. The MT-Associated Protein TPX2 Participates in Many Aspects of Spindle Assembly

Identification of TPX2 (Targeting Protein for Xklp2)
The first identification of TPX2, as its name suggests, was as a *t*argeting *p*rotein for *X*klp2, a mitotic kinesin important for pole-separation and semi-redundant with Eg5 (Wittmann et al., 1998; 2000; Vanneste et al., 2009). TPX2 showed robust spindle pole localization dependent on the activity of the motor dynein, and depletion from extract resulted in many pole-formation defects. Interestingly, overexpression of TPX2 prevented spindle formation, but resulted in increased MT density and ectopic aster formation (Wittmann et al., 2000), suggesting a role in MT nucleation.

TPX2 is Ran-regulated and Involved in MT Nucleation
After the discovery that spindle formation could be induced by DNA alone (Heald et al., 1996), the mediator of this effect was soon determined to be the small GTPase Ran, a protein previously only appreciated for its role in nucleocytoplasmic transport. Ran remains in the GTP-bound state near the DNA by the action of its nucleotide exchange factor, RCC1, which is localized to chromatin. By engineering Ran mutants with constitutive or depressed activity, several groups showed that Ran was not only necessary for spindle assembly, but that addition of active Ran caused ectopic MT nucleation (Carazo-Salas *et al.*, 1999; Kalab *et al.*, 1999; Ohba *et al.*, 1999; Wilde *et al.*, 1999; Zhang *et al.*, 1999). While the precise downstream mechanisms are still unclear, Ran's characterized role in nuclear transport provided a simple model for the function of Ran in mitosis. Transport molecules, like importin α and β, normally import cargoes by binding them in the cytoplasm and specifically releasing them in the nucleus upon binding to RanGTP, which is present in high concentrations selectively in the nucleus due to the presence of RCC1. In mitosis, importins bind cargoes in the cytoplasm, including MT-nucleating and spindle assembly factors, and specifically release them near the chromosomes where RanGTP concentration is high. The gradient of RanGTP predicted by this model that would emanate from the chromosomes has been verified with the use of FRET-based probes (Kalab et al., 2002). Several factors involved in spindle assembly have also been shown to bind importins, providing credence to this idea (Reviewed in (Walczak and Heald, 2008)).

To identify importin cargoes with MT-nucleating capacity, researchers purified cargoes from *Xenopus* egg extract by importin α binding, further fractionating them to isolate activity. The major active fraction was identified by mass spec to contain TPX2 (Gruss et al., 2001). The importin α binding sites on TPX2 have since been identified, and interestingly, unlike most cargoes, TPX2 binds to the minor binding site of importin α (Giesecke and Stewart, 2010). This atypical manner in which TPX2 binds to importin α could reduce competition by other cargoes for α binding.

Immunodepletion of TPX2 completely abrogated RanGTP-dependent MT nucleation in *Xenopus* egg extracts, and recombinant TPX2 could induce MT nucleation in solutions of pure tubulin *in vitro,* but the mechanism of its action in MT nucleation is unclear (Gruss et al., 2001; Schatz et al., 2003). This protein is predicted to have little tertiary

structure and may oligomerize, but it remains unclear whether TPX2 nucleates MTs directly or if it acts to stabilize small MT assemblies or requires other cellular factors such as the γ-TuRC for activity. Studies investigating the protein complex Augmin demonstrated an important role for TPX2 in organization of MTs during nucleation. Addition of excess Ran and TPX2 to *Xenopus* egg extracts induced the formation of MT aster structures called “fans” that emanate from minus-ends at a single point (Petry et al., 2013). Fan formation required the activity of γ-tubulin, Augmin, and TPX2, suggesting all might cooperate in MT nucleation (Figure 1.2B). This activity was also shown to reside in the c-terminal half of TPX2, and this dissertation expands upon the nucleation capacity of TPX2.

Regulation of TPX2 by Mitotic Kinases Aurora A and Polo

In addition to its roles in MT nucleation, TPX2 has been shown to have important functions at spindle poles. Aurora A is a centrosome-associated kinase whose activity is specifically triggered during mitosis and regulates downstream mitotic targets, namely by increasing centrosome nucleation (Reviewed in (Crane et al., 2012)). Aurora A itself must be phosphorylated for full activity, and TPX2 promotes this by increasing both Aurora A localization at poles and its autophosphorylation (Kufer, 2002). An unstructured n-terminal peptide tail on TPX2 (43 amino acids in human, 39 in *Xenopus*) binds to Aurora A to facilitate this interaction, and in turn, Aurora A phosphorylates TPX2 on multiple mapped sites (Kufer, 2002; Bayliss *et al.*, 2003; Eyers *et al.*, 2003; Tsai *et al.*, 2003). Also localized at the poles is the mitotic kinase Polo, a master regulator of mitosis that includes other mitotic kinases such as Aurora A as targets. One Polo phosphorylation site has been identified on TPX2 (S204), and interestingly this phosphorylation helps promote Aurora A activation (Eckerdt et al., 2009). Ultimately, though, the role and extent of these phosphorylations has not yet been determined.

TPX2 interacts with the kinesin-5 motor Eg5

While the N-terminus of TPX2 interacts with Aurora A, the C-terminal 35 amino acids have been identified as an interaction domain with Eg5 (Eckerdt et al., 2008). This interaction is necessary for the transport of TPX2 to spindle poles, suggesting Eg5 is an intermediary to interaction with dynein (Ma et al., 2010). Interestingly, it has also been shown that Eg5 targeting in the spindle requires TPX2, suggesting neither is localized to the pole without the other. Furthermore, these 35 amino acids are sufficient to bind and inhibit Eg5 motor activity *in vitro* (Ma et al., 2011). Disruptions in TPX2 and Eg5 interaction causes pole defects and buckled MTs, and as a result, the prevailing theory is that TPX2 acts to antagonize and regulate MT sliding by Eg5 (Ma et al., 2011).

An alternative explanation, or perhaps just an elaboration on the original hypothesis, is that TPX2 dynamically regulates Eg5 localization, and therefore activity (Gable et al., 2012). When Eg5 is localized at the site of anti-parallel overlaps, as in the central spindle or spindle mid-zone during anaphase, its activity is primarily to slide MTs outward. However, at the poles, where most MTs are parallel, the tetrameric motor heads of Eg5 would statically cross-link MTs. This dissertation provides support of this hypothesis and further suggests that these changes result in spindle architecture differences.

Current understanding of TPX2 contribution to spindle architecture
Despite the many activities and interactions outlined above, the cohesive contribution of TPX2 to spindle architecture is unclear. Attempts to further clarify the roles, with domain mutants for example, have not been definitive. The N-terminus, which binds Aurora A and has MT nucleating and binding activity *in vitro*, does not substitute for endogenous full-length TPX2. The C-terminus, which does not bind or nucleate MTs, can rescue MT nucleation and spindle defects in TPX2-depleted situations (Brunet et al., 2004). This conflict between *in vitro* and *in vivo* data implies a much more complex regulation of this protein in the cell and indicates that perhaps its many interacting partners help confer many of the spindle-associated activities we observe.

Aside from the pole formation activities mentioned above, TPX2 has been implicated in other areas of spindle architecture determination. In studying the importance of the Aurora A- TPX2 interaction, it was found that disrupting the binding of these two proteins resulted in short spindles, presumably by lack of MT mass nucleated near chromosomes and reduced pole separation (Bird and Hyman, 2008). Consistent with this idea, in *C. elegans* treated with RNAi for TPXL, spindles were of reduced length. The researchers supported a model whereby the amount of TPX2 loaded at the centrosome correlates positively with the length of the spindle (Greenan et al., 2010). In *Drosophila*, the closest TPX2 relative is called ssp1, for its *s*hort *sp*indle phenotype in RNAi knockdown (Goshima et al., 2007; Goshima, 2011).

An important point to note, however, is that TPX2 is not well-conserved. There is no yeast homolog, and there is significant lack of homology between metazoans. Many of the interaction domains for proteins named previously are completely absent in some species. For example, *C. elegans* TPXL is smaller and homologous with the N-terminal half of the TPX2 protein found in vertebrates and lacks the canonical Eg5 interaction domain (Karsenti, 2005). The *Drosophila* ssp1 maintains 3 of the highly conserved (but functionally not described) regions, but neither the Aurora A or Eg5 interaction domain (Goshima, 2011).

Here we present evidence that TPX2 may serve to regulate spindle length and MT distribution in *Xenopus*. While this stands in contrast to current knowledge of TPX2, it perhaps just explores the other end of the spectrum in which TPX2 activity becomes unchecked. At best, the current knowledge on TPX2 is piecemeal, and at worst it is contradictory and unclear. This work attempts to separate and clarify many of the roles of TPX2 in spindle assembly and maintenance and ultimately suggests that evolution of TPX2 orthologs that retain different activities of TPX2 could act to fine tune spindle architecture.

References

Ban, K. H., Torres, J. Z., Miller, J. J., Mikhailov, A., Nachury, M. V., Tung, J. J., Rieder, C. L., and Jackson, P. K. (2007). The END network couples spindle pole assembly to inhibition of the anaphase-promoting complex/cyclosome in early mitosis. Dev. Cell *13*, 29–42.

Bayliss, R., Sardon, T., Vernos, I., and Conti, E. (2003). Structural basis of Aurora-A activation by TPX2 at the mitotic spindle. Mol Cell *12*, 851–862.

Bird, A. W., and Hyman, A. A. (2008). Building a spindle of the correct length in human cells requires the interaction between TPX2 and Aurora A. J Cell Biol *182*, 289–300.

Brown, K. S., Blower, M. D., Maresca, T. J., Grammer, T. C., Harland, R. M., and Heald, R. (2007). Xenopus tropicalis egg extracts provide insight into scaling of the mitotic spindle. J Cell Biol *176*, 765–770.

Brunet, S., Sardon, T., Zimmerman, T., Wittmann, T., Pepperkok, R., Karsenti, E., and Vernos, I. (2004). Characterization of the TPX2 Domains Involved in Microtubule Nucleation and Spindle Assembly in Xenopus Egg Extracts. Mol. Biol. Cell *15*, 5318–5328.

Cameron, L. A., Yang, G., Cimini, D., Canman, J. C., Kisurina-Evgenieva, O., Khodjakov, A., Danuser, G., and Salmon, E. D. (2006). Kinesin 5-independent poleward flux of kinetochore microtubules in PtK1 cells. J Cell Biol *173*, 173–179.

Carazo-Salas, R. E., Guarguaglini, G., Gruss, O. J., Segref, A., Karsenti, E., and Mattaj, I. W. (1999). Generation of GTP-bound Ran by RCC1 is required for chromatin-induced mitotic spindle formation. Nature *400*, 178–181.

Chrétien, D., Metoz, F., Verde, F., Karsenti, E., and Wade, R. H. (1992). Lattice defects in microtubules: protofilament numbers vary within individual microtubules. J Cell Biol *117*, 1031–1040.

Cole, D. G., Saxton, W. M., Sheehan, K. B., and Scholey, J. M. (1994). A “slow” homotetrameric kinesin-related motor protein purified from Drosophila embryos. J Biol Chem *269*, 22913–22916.

Colombié, N., Cullen, C. F., Brittle, A. L., Jang, J. K., Earnshaw, W. C., Carmena, M., McKim, K., and Ohkura, H. (2008). Dual roles of Incenp crucial to the assembly of the acentrosomal metaphase spindle in female meiosis. Development *135*, 3239–3246.

Compton, D. A. (1998). Focusing on spindle poles. J Cell Sci *111 (Pt 11)*, 1477–1481.

Crane, R., Gadea, B., Littlepage, L., Wu, H., and Ruderman, J. V. (2012). Aurora A, Meiosis and Mitosis. Biology of the Cell *96*, 215–229.

Downing, K. H., and Nogales, E. (1998). Tubulin and microtubule structure. Curr Opin

Cell Biol *10*, 16–22.

Eckerdt, F., Eyers, P. A., Lewellyn, A. L., Prigent, C., and Maller, J. L. (2008). Spindle pole regulation by a discrete Eg5-interacting domain in TPX2. Curr Biol *18*, 519–525.

Eckerdt, F., Pascreau, G., Phistry, M., Lewellyn, A. L., DePaoli-Roach, A. A., and Maller, J. L. (2009). Phosphorylation of TPX2 by Plx1 enhances activation of Aurora A. Cell Cycle *8*, 2413–2419.

Endow, S. A., Chandra, R., Komma, D. J., Yamamoto, A. H., and Salmon, E. D. (1994). Mutants of the Drosophila ncd microtubule motor protein cause centrosomal and spindle pole defects in mitosis. J Cell Sci *107 (Pt 4)*, 859–867.

Eyers, P. A., Erikson, E., Chen, L. G., and Maller, J. L. (2003). A novel mechanism for activation of the protein kinase Aurora A. Curr Biol *13*, 691–697.

Gable, A. *et al.* (2012). Dynamic reorganization of Eg5 in the mammalian spindle throughout mitosis requires dynein and TPX2. Mol. Biol. Cell *23*, 1254–1266.

Gadea, B. B., and Ruderman, J. V. (2005). Aurora kinase inhibitor ZM447439 blocks chromosome-induced spindle assembly, the completion of chromosome condensation, and the establishment of the spindle integrity checkpoint in Xenopus egg extracts. Mol. Biol. Cell *16*, 1305–1318.

Gadea, B. B., and Ruderman, J. V. (2006). Aurora B is required for mitotic chromatin-induced phosphorylation of Op18/Stathmin. Proc Natl Acad Sci USA *103*, 4493–4498.

Giesecke, A., and Stewart, M. (2010). Novel Binding of the Mitotic Regulator TPX2 (Target Protein for Xenopus Kinesin-like Protein 2) to Importin. Journal of Biological Chemistry *285*, 17628–17635.

Goshima, G. (2011). Identification of a TPX2-like microtubule-associated protein in Drosophila. PLoS ONE *6*, e28120.

Goshima, G., Mayer, M., Zhang, N., Stuurman, N., and Vale, R. D. (2008). Augmin: a protein complex required for centrosome-independent microtubule generation within the spindle. J Cell Biol *181*, 421–429.

Goshima, G., Wollman, R., Goodwin, S. S., Zhang, N., Scholey, J. M., Vale, R. D., and Stuurman, N. (2007). Genes required for mitotic spindle assembly in Drosophila S2 cells. Science *316*, 417–421.

Greenan, G., Brangwynne, C. P., Jaensch, S., Gharakhani, J., Jülicher, F., and Hyman, A. A. (2010). Centrosome size sets mitotic spindle length in Caenorhabditis elegans embryos. Curr Biol *20*, 353–358.

Gruss, O. J., Carazo-Salas, R. E., Schatz, C. A., Guarguaglini, G., Kast, J., Wilm, M., Le Bot, N., Vernos, I., Karsenti, E., and Mattaj, I. W. (2001). Ran induces spindle assembly

by reversing the inhibitory effect of importin alpha on TPX2 activity. Cell *104*, 83–93.

Guillet, V. *et al.* (2011). Crystal structure of γ-tubulin complex protein GCP4 provides insight into microtubule nucleation. Nat Struct Mol Biol *18*, 915–919.

Halpin, D., Kalab, P., Wang, J., Weis, K., and Heald, R. (2011). Mitotic spindle assembly around RCC1-coated beads in Xenopus egg extracts. PLoS Biol *9*, e1001225.

Hannak, E., Oegema, K., Kirkham, M., Gönczy, P., Habermann, B., and Hyman, A. A. (2002). The kinetically dominant assembly pathway for centrosomal asters in Caenorhabditis elegans is gamma-tubulin dependent. J Cell Biol *157*, 591–602.

Heald, R., Tournebize, R., Blank, T., Sandaltzopoulos, R., Becker, P., Hyman, A., and Karsenti, E. (1996). Self-organization of microtubules into bipolar spindles around artificial chromosomes in Xenopus egg extracts. Nature *382*, 420–425.

Helmke, K. J., Heald, R., and Wilbur, J. D. (2013). Interplay between spindle architecture and function. Int Rev Cell Mol Biol *306*, 83–125.

Holy, T. E., and Leibler, S. (1994). Dynamic instability of microtubules as an efficient way to search in space. Proc Natl Acad Sci USA *91*, 5682–5685.

Jensen, C. G. (1982). Dynamics of spindle microtubule organization: kinetochore fiber microtubules of plant endosperm. J Cell Biol *92*, 540–558.

Kalab, P., Pu, R. T., and Dasso, M. (1999). The ran GTPase regulates mitotic spindle assembly. Curr Biol *9*, 481–484.

Kalab, P., Weis, K., and Heald, R. (2002). Visualization of a Ran-GTP Gradient in Interphase and Mitotic Xenopus Egg Extracts. Science *295*, 2452–2456.

Kapoor, T. M., Mayer, T. U., Coughlin, M. L., and Mitchison, T. J. (2000). Probing spindle assembly mechanisms with monastrol, a small molecule inhibitor of the mitotic kinesin, Eg5. J Cell Biol *150*, 975–988.

Karsenti, E. (2005). TPX or Not TPX? Mol Cell *19*, 431–432.

Khodjakov, A. (2003). Minus-end capture of preformed kinetochore fibers contributes to spindle morphogenesis. J Cell Biol *160*, 671–683.

Khodjakov, A., Cole, R. W., Oakley, B. R., and Rieder, C. L. (2000). Centrosome-independent mitotic spindle formation in vertebrates. Curr Biol *10*, 59–67.

Kollman, J. M., Merdes, A., Mourey, L., and Agard, D. A. (2011). Microtubule nucleation by γ-tubulin complexes. Nat Rev Mol Cell Biol *12*, 709–721.

Kollman, J. M., Polka, J. K., Zelter, A., Davis, T. N., and Agard, D. A. (2010).

Microtubule nucleating gamma-TuSC assembles structures with 13-fold microtubule-like symmetry. Nature *466*, 879–882.

Kollu, S., Bakhoum, S. F., and Compton, D. A. (2009). Interplay of microtubule dynamics and sliding during bipolar spindle formation in mammalian cells. Curr Biol *19*, 2108–2113.

Kraft, C., Herzog, F., Gieffers, C., Mechtler, K., Hagting, A., Pines, J., and Peters, J.-M. (2003). Mitotic regulation of the human anaphase-promoting complex by phosphorylation. Embo J *22*, 6598–6609.

Kufer, T. A., Silljé, H. H. W., Körner, R., Gruss, O. J., meraldi, P., and Nigg, E. A. (2002). Human TPX2 is required for targeting Aurora-A kinase to the spindle. J Cell Biol *158*, 617–623.

Loughlin, R., Wilbur, J. D., McNally, F. J., Nédélec, F. J., and Heald, R. (2011). Katanin Contributes to Interspecies Spindle Length Scaling in Xenopus. Cell *147*, 1397–1407.

Ma, N., Titus, J., Gable, A., Ross, J. L., and Wadsworth, P. (2011). TPX2 regulates the localization and activity of Eg5 in the mammalian mitotic spindle. J Cell Biol *195*, 87–98.

Ma, N., Tulu, U. S., Ferenz, N. P., Fagerstrom, C., Wilde, A., and Wadsworth, P. (2010). Poleward transport of TPX2 in the mammalian mitotic spindle requires dynein, Eg5, and microtubule flux. Mol. Biol. Cell *21*, 979–988.

Mahoney, N. M., Goshima, G., Douglass, A. D., and Vale, R. D. (2006). Making Microtubules and Mitotic Spindles in Cells without Functional Centrosomes. Current Biology *16*, 564–569.

Maiato, H., Rieder, C. L., and Khodjakov, A. (2004). Kinetochore-driven formation of kinetochore fibers contributes to spindle assembly during animal mitosis. J Cell Biol *167*, 831–840.

Maresca, T. J., and Heald, R. (2006). Methods for studying spindle assembly and chromosome condensation in Xenopus egg extracts. Methods Mol. Biol. *322*, 459–474.

Merdes, A., Heald, R., Samejima, K., Earnshaw, W. C., and Cleveland, D. W. (2000). Formation of spindle poles by dynein/dynactin-dependent transport of NuMA. J Cell Biol *149*, 851–862.

Mitchison, T. J., and Kirschner, M. W. (1985). Properties of the kinetochore in vitro. I. Microtubule nucleation and tubulin binding. J Cell Biol *101*, 755–765.

Mitchison, T., and Kirschner, M. (1984a). Dynamic instability of microtubule growth. Nature *312*, 237–242.

Mitchison, T., and Kirschner, M. (1984b). Microtubule assembly nucleated by isolated centrosomes. Nature *312*, 232–237.

Miyamoto, D. T., Perlman, Z. E., Burbank, K. S., Groen, A. C., and Mitchison, T. J. (2004). The kinesin Eg5 drives poleward microtubule flux in Xenopus laevis egg extract spindles. J Cell Biol *167*, 813–818.

Ohba, T., Nakamura, M., Nishitani, H., and Nishimoto, T. (1999). Self-organization of microtubule asters induced in Xenopus egg extracts by GTP-bound Ran. Science *284*, 1356–1358.

Ohi, R., Sapra, T., Howard, J., and Mitchison, T. J. (2004). Differentiation of cytoplasmic and meiotic spindle assembly MCAK functions by Aurora B-dependent phosphorylation. Mol. Biol. Cell *15*, 2895–2906.

Paul, R., Wollman, R., Silkworth, W. T., Nardi, I. K., Cimini, D., and Mogilner, A. (2009). Computer simulations predict that chromosome movements and rotations accelerate mitotic spindle assembly without compromising accuracy. Proc Natl Acad Sci USA *106*, 15708–15713.

Pepper, D. A., and Brinkley, B. R. (1979). Microtubule initiation at kinetochores and centrosomes in lysed mitotic cells. Inhibition of site-specific nucleation by tubulin antibody. J Cell Biol *82*, 585–591.

Petry, S., Groen, A. C., Ishihara, K., Mitchison, T. J., and Vale, R. D. (2013). Branching Microtubule Nucleation in Xenopus Egg Extracts Mediated by Augmin and TPX2. Cell *152*, 768–777.

Petry, S., Pugieux, C., Nedelec, F. J., and Vale, R. D. (2011). Augmin promotes meiotic spindle formation and bipolarity in Xenopus egg extracts. Proceedings of the National Academy of Sciences *108*, 14473–14478.

Rieder, C. L. (2005). Kinetochore fiber formation in animal somatic cells: dueling mechanisms come to a draw. Chromosoma *114*, 310–318.

Ruchaud, S., Carmena, M., and Earnshaw, W. C. (2007). Chromosomal passengers: conducting cell division. Nat Rev Mol Cell Biol *8*, 798–812.

Sampath, S. C., Ohi, R., Leismann, O., Salic, A., Pozniakovski, A., and Funabiki, H. (2004). The Chromosomal Passenger Complex Is Required for Chromatin-Induced Microtubule Stabilization and Spindle Assembly. Cell *118*, 187–202.

Schatz, C. A., Santarella, R., Hoenger, A., Karsenti, E., Mattaj, I. W., Gruss, O. J., and Carazo-Salas, R. E. (2003). Importin alpha-regulated nucleation of microtubules by TPX2. Embo J *22*, 2060–2070.

Somma, M. P. *et al.* (2008). Identification of Drosophila mitotic genes by combining co-expression analysis and RNA interference. PLoS Genet *4*, e1000126.

Song, L., and Rape, M. (2010). Regulated degradation of spindle assembly factors by the anaphase-promoting complex. Mol Cell *38*, 369–382.

Tirnauer, J. S., Salmon, E. D., and Mitchison, T. J. (2004). Microtubule plus-end dynamics in Xenopus egg extract spindles. Mol. Biol. Cell *15*, 1776–1784.

Torosantucci, L., De Luca, M., Guarguaglini, G., Lavia, P., and Degrassi, F. (2008). Localized RanGTP accumulation promotes microtubule nucleation at kinetochores in somatic mammalian cells. Mol. Biol. Cell *19*, 1873–1882.

Tsai, M.-Y., Wiese, C., Cao, K., Martin, O., Donovan, P., Ruderman, J., Prigent, C., and Zheng, Y. (2003). A Ran signalling pathway mediated by the mitotic kinase Aurora A in spindle assembly. Nat Cell Biol *5*, 242–248.

Tugendreich, S., Tomkiel, J., Earnshaw, W., and Hieter, P. (1995). CDC27Hs colocalizes with CDC16Hs to the centrosome and mitotic spindle and is essential for the metaphase to anaphase transition. Cell *81*, 261–268.

Tulu, U. S., Fagerstrom, C., Ferenz, N. P., and Wadsworth, P. (2006). Molecular requirements for kinetochore-associated microtubule formation in mammalian cells. Curr Biol *16*, 536–541.

Uehara, R., Nozawa, R. S., Tomioka, A., Petry, S., Vale, R. D., Obuse, C., and Goshima, G. (2009). The augmin complex plays a critical role in spindle microtubule generation for mitotic progression and cytokinesis in human cells. Proceedings of the National Academy of Sciences *106*, 6998–7003.

Uteng, M., Hentrich, C., Miura, K., Bieling, P., and Surrey, T. (2008). Poleward transport of Eg5 by dynein-dynactin in Xenopus laevis egg extract spindles. J Cell Biol *182*, 715–726.

Vanneste, D., Takagi, M., Imamoto, N., and Vernos, I. (2009). The Role of Hklp2 in the Stabilization and Maintenance of Spindle Bipolarity. Current Biology *19*, 1712–1717.

Walczak, C. E., and Heald, R. (2008). Mechanisms of Mitotic Spindle Assembly and Function. In: International Review of Cytology, Elsevier, 111–158.

Wilde, A., and Zheng, Y. (1999). Stimulation of microtubule aster formation and spindle assembly by the small GTPase Ran. Science *284*, 1359–1362.

Williamson, A., Wickliffe, K. E., Mellone, B. G., Song, L., Karpen, G. H., and Rape, M. (2009). Identification of a physiological E2 module for the human anaphase-promoting complex. Proceedings of the National Academy of Sciences *106*, 18213–18218.

Wittmann, T., Boleti, H., Antony, C., Karsenti, E., and Vernos, I. (1998). Localization of the kinesin-like protein Xklp2 to spindle poles requires a leucine zipper, a microtubule-associated protein, and dynein. J Cell Biol *143*, 673–685.

Wittmann, T., Wilm, M., Karsenti, E., and Vernos, I. (2000). TPX2, A novel xenopus MAP involved in spindle pole organization. J Cell Biol *149*, 1405–1418.

Wollman, R., Cytrynbaum, E. N., Jones, J. T., and Meyer, T. (2005). Efficient chromosome capture requires a bias in the “search-and-capture”process during mitotic-spindle assembly. Current Biology.

Wu, J. Q., and Kornbluth, S. (2008). Across the meiotic divide - CSF activity in the post-Emi2/XErp1 era. J Cell Sci *121*, 3509–3514.

Zhang, C., Hughes, M., and Clarke, P. R. (1999). Ran-GTP stabilises microtubule asters and inhibits nuclear assembly in Xenopus egg extracts. J Cell Sci *112 (Pt 14)*, 2453–2461.

Chapter 2: TPX2 Levels Modulate Meiotic Spindle Size and Microtubule Distribution in *Xenopus* Egg Extracts

Background

The function of the spindle to accurately segregate chromosomes during cell division is universal among eukaryotes. A common feature of metaphase spindles is their bipolar structure, with microtubule (MT) minus ends pointing toward the poles, and MT plus ends toward the center, with a subset of them connecting to chromosomes at the kinetochores. However, wide variation in spindle assembly, size and morphology is observed among different cell types, presumably to optimize spindle function (Goshima *et al.*, 2005; Helmke *et al.*, 2013). For example, in cultured somatic cells centrosomes serve as the dominant MT nucleating sites at each spindle pole that direct spindle formation and also generate astral MTs that function in spindle positioning, whereas meiotic spindles of eggs and oocytes frequently lack centrosomes and astral MT arrays and assemble by self-organization of MTs stabilized by chromatin. It is now accepted that spindles form through a combination of mechanisms, but how a particular spindle architecture is established and contributes to spindle function is poorly understood.

Xenopus provides a valuable system to study a variety of spindle types *in vitro*, since spindles formed in egg and embryo extracts recapitulate morphologies observed *in vivo*. The ellipsoidal, ~35 μm long *Xenopus laevis* meiotic spindle has been studied most extensively and is thought to be built from a tiled array of dynamic, overlapping MTs generated by a gradient of RanGTP around chromatin and organized by motor proteins (Yang *et al.*, 2008; Loughlin *et al.*, 2010; Needleman *et al.*, 2010; Brugués *et al.*, 2012). Meiotic spindles assembled in egg extracts of the smaller *Xenopus tropicalis* frog possess a similar anastral appearance but are significantly shorter at ~22 μm (Brown *et al.*, 2007). *In vitro* spindle size scaling can also be seen by comparing mitotic spindles assembled in extracts from *X. laevis* embryos containing four large cells at stage 3 to extracts prepared from 4000 small cells at stage 8 (Wilbur and Heald, 2013). In both interspecies and developmental spindle scaling, modulation of the activity of factors that destabilize MTs contributed to differences in spindle lengths (Loughlin *et al.*, 2011; Wilbur and Heald, 2013). Also apparent among these spindles were differences in morphology and the apparent role of centrosomes and kinetochores in spindle assembly and organization. Although centrosomes were present in both mitotic spindle types, connections between centrosome-nucleated MTs and chromosomes were more prominent in the smaller stage 8 spindles, which unlike the larger stage 3 spindles were not disrupted by RanGTP inhibition (Wilbur and Heald, 2013). Compared to the larger *X. laevis* spindles, *X. tropicalis* spindles contained more robust kinetochore fibers that required greater MT destabilizing activity to contain them within the spindle (Loughlin *et al.*, 2011).

Although a large number of factors have been identified that could contribute to differences in spindle assembly and architecture, the molecular basis of differences in spindle morphology is unknown. Here we focused on the conserved MT-associated protein TPX2, which interacts with several key spindle regulators and possesses a variety of activities that make it central to spindle assembly. Originally identified as the

spindle-targeting factor for the kinesin motor Xklp2 in *Xenopus* (Wittmann *et al.*, 2000), TPX2 is a Ran-regulated cargo of the transport factor importin α and a major activity driving chromatin-mediated MT nucleation (Gruss *et al.*, 2001; Schatz *et al.*, 2003). Interaction of TPX2 with the mitotic kinase Aurora A is required to establish appropriate spindle length in human cells (Bird and Hyman, 2008), and a gradient of the TPX2-like (TPXL) protein emanating from the centrosome correlates with spindle length In *C. elegans* embryos (Greenan *et al.*, 2010). TPX2 is also known to interact with the kinesin-5 Eg5, a homotetrameric plus-end directed motor that can bind and cross-link two MTs (Cole *et al.*, 1994). Eg5 preferentially binds antiparallel MTs *in vitro* (van den Wildenberg *et al.*, 2008), sliding them apart, and this activity serves to promote the proper arrangement of MTs in the spindle with their plus-ends directed toward the spindle center and minus-ends extending outward, as well as spindle bipolarity, elongation and poleward MT flux, (Sawin *et al.*, 1992; Walczak *et al.*, 1998; Kapoor *et al.*, 2000; Miyamoto *et al.*, 2004). *In vivo*, Eg5 is frequently observed to be enriched at spindle poles, where it would bundle parallel MTs. TPX2 not only contributes to Eg5 localization, but directly inhibits Eg5 motility *in vitro* (Ma *et al.*, 2010; 2011; Gable *et al.*, 2012). Its many interactions and functions demonstrate a crucial role for TPX2 in spindle formation, but how it contributes to spindle architecture is not understood.

Taking advantage of the interspecies egg extract system comparing *X. laevis* and *X. tropicalis* meiotic spindles, we show here that TPX2 levels and activity regulate basic features of spindle architecture including size, dependency on the Ran pathway, MT nucleation, and organization by MT motor proteins. We propose that TPX2 modulates spindle structure in part by partitioning Eg5 between tiled anti-parallel MTs and polar parallel MT arrays. These results indicate that small variations in the interactions of a common set of spindle assembly factors define distinct architectures in small and large spindles.

Results

X. tropicalis and *X. laevis* egg extract spindles are architecturally distinct

We showed previously that spindles formed in *X. tropicalis* egg extracts are smaller than those in *X. laevis* and contain more stable kinetochore fibers (Loughlin *et al.*, 2011). Upon live imaging single planes at higher resolution with spinning disk confocal, we also observed that whereas *X. laevis* spindles contained highly bundled MTs that extended continuously from pole-to-pole, *X. tropicalis* spindles lacked MT density in the midzone (Figure 2.1), suggesting a different overall architecture than the overlapping tiled MT array characteristic of *X. laevis* meiotic spindles, which had not previously been appreciated in fixed spindles or at lower resolution (Yang *et al.*, 2008; Loughlin *et al.*, 2010; Needleman *et al.*, 2010; Brugués *et al.*, 2012).

To determine whether this difference in MT distribution reflected a change in chromatin-mediated MT nucleation, we disrupted the RanGTP pathway by adding a dominant-negative mutant, RanT24N, which completely abolishes spindle formation in *X. laevis* egg extracts (Kalab *et al.*, 1999). Surprisingly, even at RanT24N levels 20-fold higher than that required to disrupt *X. laevis*, *X. tropicalis* extracts assembled bipolar spindles (Figure 2.2A; Figure 2.5B). We found that disrupting the Ran pathway by adding the cargo-binding domain of importin-β gave similar results, although the existence of the RanGTP gradient in *X. tropicalis* could be verified with FRET-based sensors (Figure 2.2, C and D; Nachury *et al.*, 2001; Kalab *et al.*, 2002). Interestingly, Ran pathway inhibition did not interfere with spindle localization of the downstream importin-α cargo TPX2 (Figure 2.2, A and B). These results suggest that, unlike for *X. laevis*, the RanGTP gradient is not necessary for meiotic spindle formation and release of spindle assembly cargoes from importins in *X. tropicalis* egg extracts.

Figure 2.1

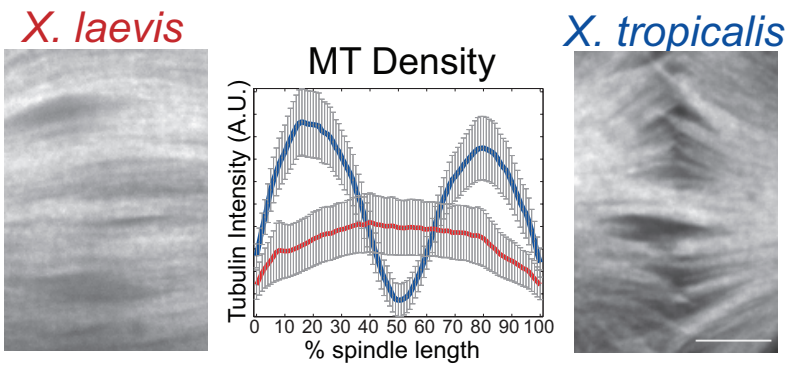

Figure 2.1 *X. tropicalis* and *X. laevis* spindles differ in morphology
Spinning disk confocal images of *X. laevis* and *X. tropicalis* spindle midzones in live spindle reactions on PEG-coated glass. Scale bar 5 μm. Average linescan intensity of MTs across the length of the spindle (as described in Materials and Methods), showing reduced MT density in the center of the spindle of *X. tropicalis*, n=15 spindles for *X. laevis* and n=19 for *X. tropicalis* from 3 extracts.

Figure 2.2

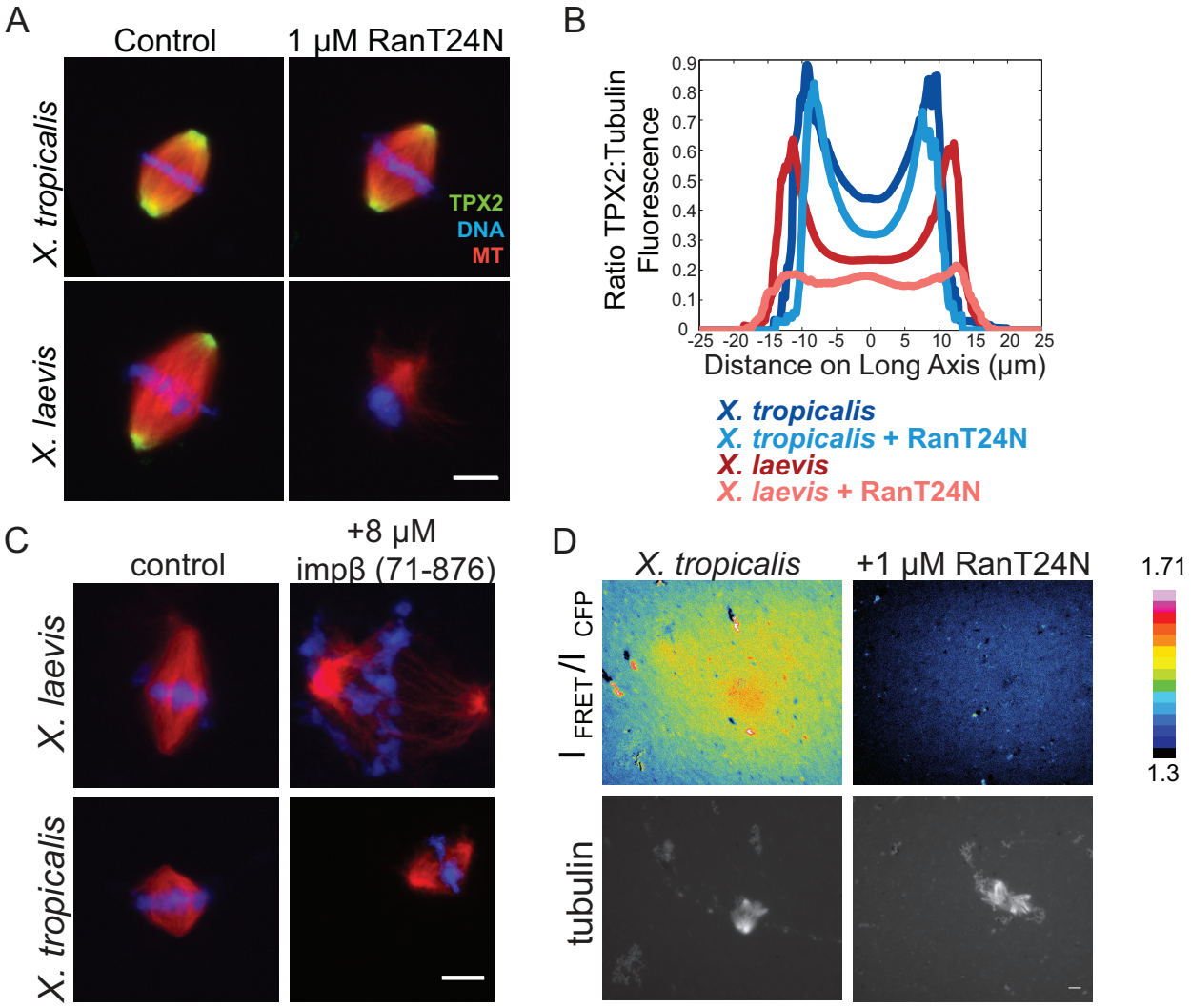
A
Control
1 μM RanT24N
X. tropicalis
X. laevis
TPX2
DNA
MT
B
Ratio TPX2:Tubulin Fluorescence
0.9
0.8
0.7
0.6
0.5
0.4
0.3
0.2
0.1
0
-25 -20 -15 -10 -5 0 5 10 15 20 25
Distance on Long Axis (μm)
X. tropicalis
X. tropicalis + RanT24N
X. laevis
X. laevis + RanT24N
C
control
+8 μM impβ (71-876)
X. laevis
X. tropicalis
D
X. tropicalis
+1 μM RanT24N
I FRET/I CFP
tubulin
1.71
1.3

Figure 2.2 *X. tropicalis* and *X. laevis* spindles differ in sensitivity to inhibition of Ran

(A) Inhibition of the RanGTP pathway with 1 μM of the dominant-negative mutant RanT24N disrupted spindle assembly in *X. laevis* but not *X. tropicalis* egg extracts. Scale bar 10 μm.

(B) Line scan quantification of TPX2 immunofluorescence relative to tubulin intensity from >50 spindles in each condition from one representative experiment. TPX2 intensity was higher in *X. tropicalis* spindles (dark blue) and remained unchanged upon addition of 5 μM RanT24N (light blue), while *X. laevis* spindles recruited less TPX2 (red) which was lost upon RanT24N treatment (pink).

(C) Inhibition of the RanGTP pathway with 8 μM of the importin beta cargo binding domain (71-876) disrupted spindle assembly in *X. laevis* but not *X. tropicalis* egg extracts. Scale bar 10 μm.

(D) Visualization of RanGTP gradient in *X. tropicalis* spindles using 1 μM of the Rango FRET probe (Kaláb et al., 2006). FRET efficiency shown by I_{FRET}/I_{CFP}. 1 μM RanT24N treatment abolished this gradient, but spindle assembly still occurs, as seen by the presence of MT structures. Scale bar 10 μm.

Consistent with a decreased dependence on the Ran pathway in *X. tropicalis* egg extracts, addition of a constitutively GTP-bound mutant, RanQ69L, which induces ectopic MT nucleation and formation of bipolar “mini spindles” lacking DNA in *X. laevis* extracts (Carazo-Salas *et al.*, 1999; Kalab *et al.*, 1999; Ohba *et al.*, 1999; Wilde and Zheng, 1999; Zhang *et al.*, 1999) failed to induce similar structures in *X. tropicalis* (Figure 2.3A). These observations indicated that *X. tropicalis* spindle organization and bipolarity might arise from alternative mechanisms. We therefore compared the effects of monastrol, a small molecule inhibitor of Eg5, to evaluate its importance for bipolar spindle formation in the two extracts. Monastrol is predicted to inhibit Eg5 comparably in both species, since its binding pocket is 94% similar, with all residues contacting the small molecule completely conserved (Maliga and Mitchison, 2006). Consistent with prior reports, adding increasing monastrol concentrations to *X. laevis* extract caused spindle shortening and collapse, generating mono-aster structures with an apparent IC50 of 21 μM (Kapoor *et al.*, 2000). Surprisingly, while *X. tropicalis* spindles shortened, they collapsed only at high concentrations of monastrol, with an IC50 of 211 μM (Figure 2.3B, Figure 2.5C). Altogether, these experiments reveal that the two *Xenopus* spindles differ significantly, not only in size, but also in architecture and assembly mechanism.

Figure 2.3

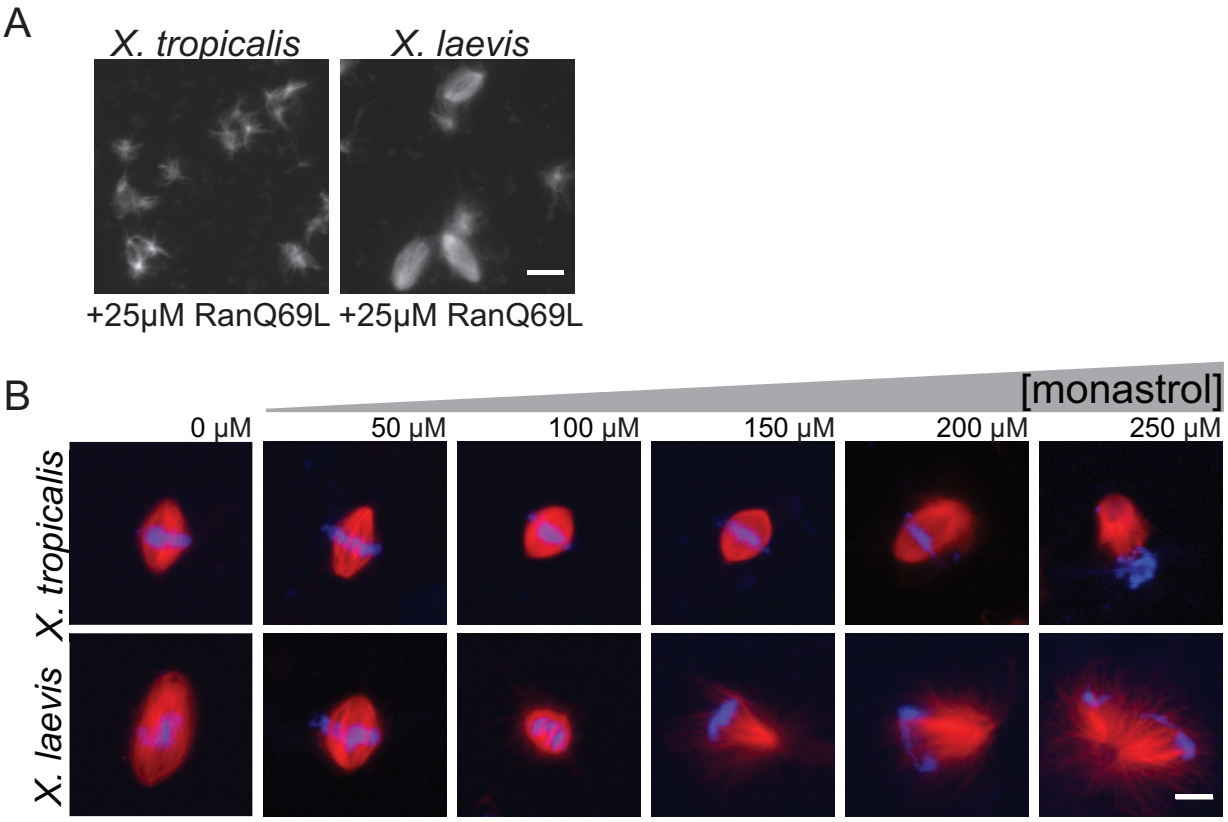

Figure 2.3 Spindle organization and bipolarity in *X. tropicalis* does not rely on Ran and Eg5

(A) Treatment of *X. laevis* and *X. tropicalis* egg extracts with 25 μM RanQ69L induced ectopic MT nucleation in both reactions, but MT organization into bipolar arrays was not seen in *X. tropicalis.* Scale bar 10 μm.

(B) Representative images of spindle assembly reactions in *X. laevis* and *X. tropicalis* egg extracts in the presence of increasing amounts of monastrol to inhibit Eg5. *X. laevis* spindles begin to shorten and collapse with increasing monastrol, while *X. tropicalis* spindles show little collapse and are resistant to monastrol except at the highest concentrations. Scale bar 10 μm.

TPX2 levels correlate with RanGTP- and Eg5-dependence and spindle size

As a Ran-regulated factor known to interact with Eg5, the MT-associated protein TPX2 was an attractive candidate for mediating differences between *X. laevis* and *X. tropicalis.* While most spindle factors tested by Western blot were found to be present in similar amounts (Figure 2.4A), TPX2 concentration was approximately 3-fold higher in *X. tropicalis* compared to *X. laevis* extracts, at ~300 nM (Figure 2.4B; Gruss *et al.*, 2001). Antibody affinity to the species orthologs was determined to be similar, suggesting this Western is an accurate measure of cytoplasmic concentration (Figure 2.4C).

To determine whether TPX2 concentration affected spindle morphology, we supplemented *X. laevis* extract with recombinant *X. laevis* TPX2 to match levels in *X. tropicalis*. Strikingly, metaphase spindle length was reduced by 20% (Figure 2.5A). Furthermore, altering TPX2 concentration in egg extracts was sufficient to change their sensitivity to inhibition of Ran and Eg5 (Figure 2.5, B and C). Depletion of TPX2 from *X. tropicalis* extracts rendered them sensitive to RanT24N, which then abolished spindle assembly. Conversely, addition of recombinant TPX2 to *X. laevis* extracts rescued spindle assembly in the presence of RanT24N (Figure 2.5B) and spindle bipolarity in the presence of higher concentrations of monastrol (Figure 2.5C). This effect required the TPX2-Eg5 interaction, as a TPX2 mutant lacking the Eg5-binding domain did not rescue monastrol sensitivity (data not shown).

In summary, TPX2 concentration appears to specify the relative importance of the RanGTP pathway and Eg5 for spindle assembly, and increasing TPX2 levels in *X. laevis* shrinks the meiotic spindle to a size similar to that of *X. tropicalis*.

Figure 2.4

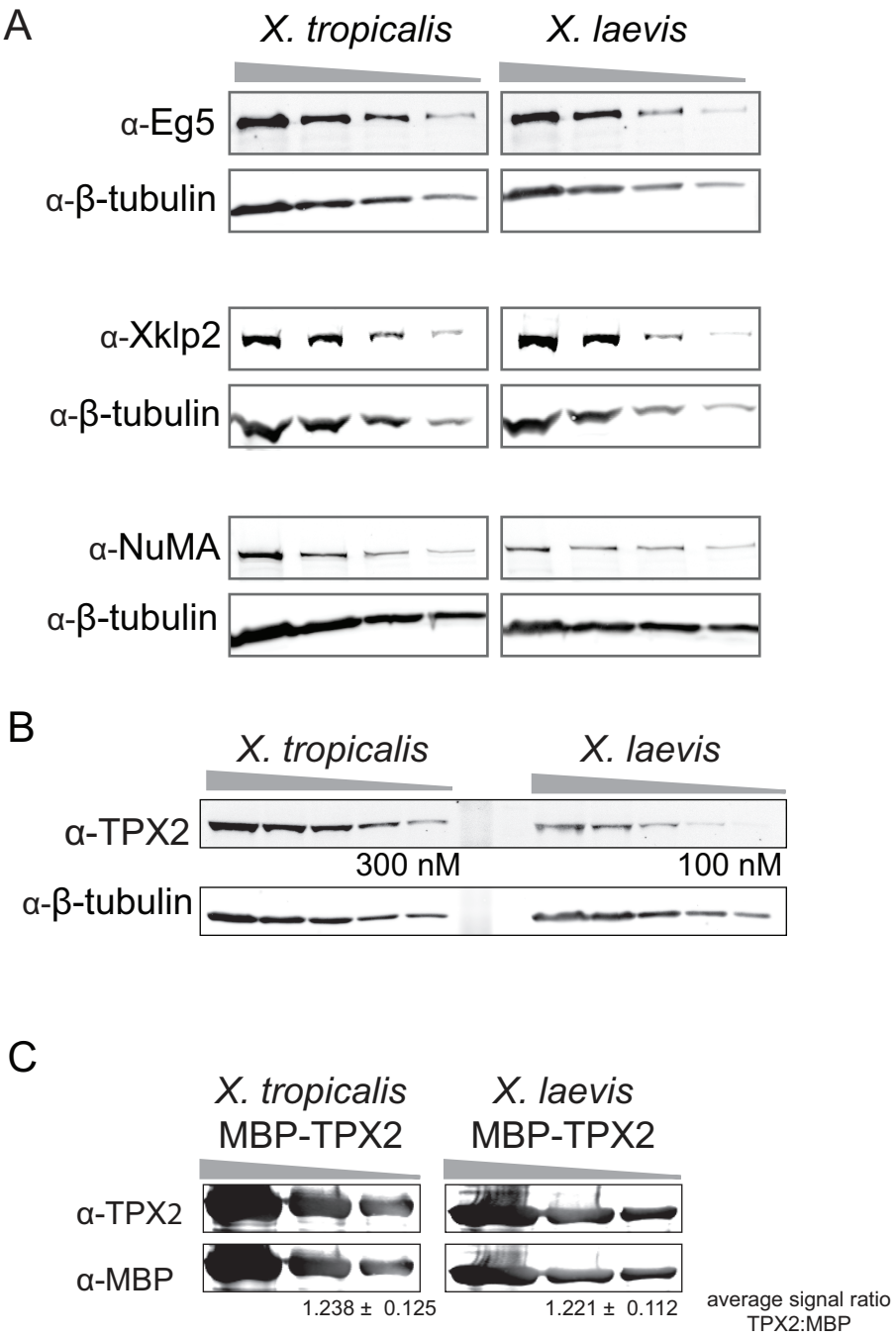
A
X. tropicalis
X. laevis
α-Eg5
α-β-tubulin
α-Xklp2
α-β-tubulin
α-NuMA
α-β-tubulin
B
X. tropicalis
X. laevis
α-TPX2
300 nM
100 nM
α-β-tubulin
C
X. tropicalis
MBP-TPX2
X. laevis
MBP-TPX2
α-TPX2
α-MBP
1.238 ± 0.125
1.221 ± 0.112
average signal ratio
TPX2:MBP

Figure 2.4 TPX2 levels are 3-fold higher in *X. tropicalis* extracts
(A) Representative Western Blot of dilution series of *X. tropicalis* and *X. laevis* egg extracts probed with antibodies for Eg5, Xklp2, or NuMA. β-tubulin is shown as a loading control. Band intensities from Western Blots of three extracts each were quantified (LI-COR Odyssey software), and on average these proteins were not different between the two extracts.

(B) Representative Western Blot of dilution series of *X. tropicalis* and *X. laevis* egg extracts showing higher levels of TPX2 present in *X. tropicalis*. β-tubulin is shown as a loading control. Band intensities from Western Blots of three extracts each were quantified (LI-COR Odyssey software), and on average were approximately 3-fold higher in *X. tropicalis* compared to *X. laevis*, giving an estimated concentration of 300 nM (*X. laevis* TPX2 concentration is ~100 nM, (Gruss *et al.*, 2001).

(C) Representative Western Blot of dilution series of recombinant *X. tropicalis* MBP-TPX2 and recombinant *X. laevis* MBP-TPX2, probed with the TPX2 antibody shown in B as well as an α-MBP antibody (New England BioLabs). Band intensities were quantified (LI-COR Odyssey software), and the signal ratio of TPX2:MBP calculated for each lane. The signal ratios were not significantly different: 1.238 ± 0.125 in *X. tropicalis* and 1.221 ± 0.112 in *X. laevis.*

Figure 2.5

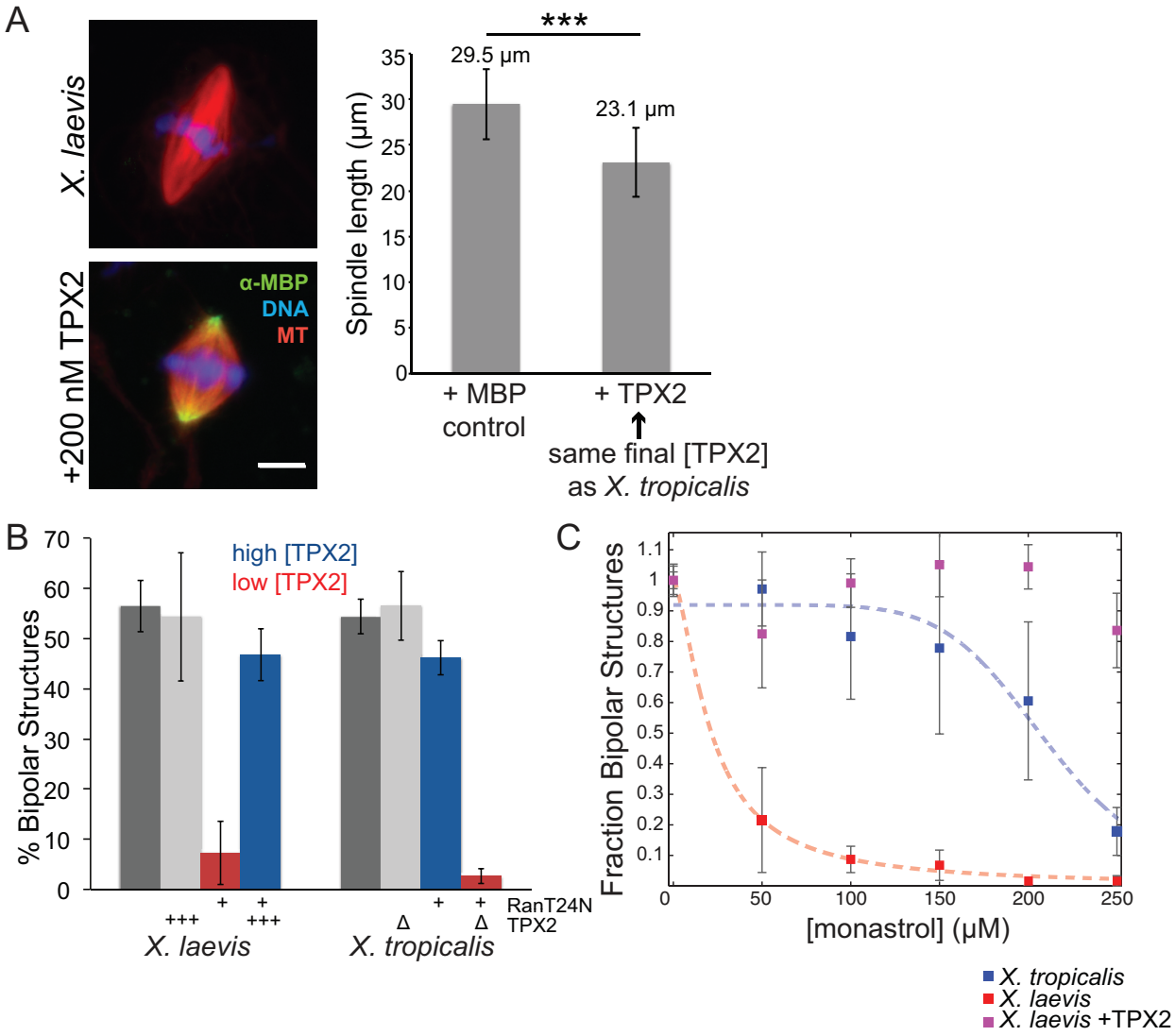
A
X. laevis
+200 nM TPX2
α-MBP
DNA
MT
***
29.5 µm
23.1 µm
Spindle length (µm)
35
30
25
20
15
10
5
0
+ MBP control
+ TPX2
same final [TPX2] as X. tropicalis
B
high [TPX2]
low [TPX2]
% Bipolar Structures
70
60
50
40
30
20
10
0
+++
+
+
+++
Δ
+
+
Δ
RanT24N
TPX2
X. laevis
X. tropicalis
C
Fraction Bipolar Structures
1.1
1
0.9
0.8
0.7
0.6
0.5
0.4
0.3
0.2
0.1
0
50
100
150
200
250
[monastrol] (µM)
X. tropicalis
X. laevis
X. laevis +TPX2

Figure 2.5 TPX2 levels correlate with RanGTP- and Eg5-dependence and spindle size

(A) Left: Addition of 200 nM MBP-TPX2 to *X. laevis* extracts decreased spindle size. Polar localization of recombinant protein is detected by immunofluorescence against the MBP tag. Scale bar 10 μm. Right: Quantification of spindle length with addition of 200 nM MBP-TPX2 compared to control of addition of 200 nM MBP. Mean ± SD, n ≥ 671 spindles in each condition from three separate extracts, $p<0.0001$ from unpaired t-test.

(B) Quantification of spindle bipolarity as an indicator of proper spindle formation upon inhibition of the RanGTP pathway in *X. laevis* and *X. tropicalis* egg extracts. For each condition, all MT structures near condensed DNA were scored for morphology with n ≥ 100 for each extract in three separate experiments. Bipolarity percent was calculated from total structures scored, mean ± SD. Dark gray bars indicate control extracts with no treatment. With 5 μM RanT24N addition, spindle formation in *X. laevis* egg extracts was impaired, and the fraction of bipolar structures decreased to 7.3% (left red bar) with the remaining structures monopolar (39%) or containing no MTs (45.8%). When *X. laevis* extracts were supplemented with 200 nM MBP-TPX2, spindle bipolarity with RanT24N treatment was strongly rescued (left blue bar). TPX2 addition alone does not affect bipolarity (left light gray bar). *X. tropicalis* only showed a modest decrease with RanT24N treatment, from 54% to 46%. (right blue bar). However, when *X. tropicalis* was immunodepleted of TPX2, bipolarity was almost completely lost upon RanT24N treatment, which reduces spindle efficiency to 2.7% (right red bar). TPX2 immunodepletion in *X. tropicalis* does not affect bipolarity (right light gray bar).

(C) Quantification of spindle bipolarity of *X. laevis*, *X. laevis* + 200 nM MBP-TPX2, and *X. tropicalis* MT structures upon monastrol treatment at the indicated concentration. MT structures were scored as in (C) but normalized to the 0 μM condition for each extract and plotted as the mean ± SE. Four-parameter logistic fit shown for both *X. tropicalis* (blue dashed line, IC50 211 μM) and *X. laevis* (red dashed line, IC50 21 μM), but no fit could be calculated for the *X. laevis* + TPX2 condition as it was resistant to monastrol treatment at the highest possible concentration.

TPX2 regulates spindle size and MT distribution through interaction with Eg5

Since TPX2-dependent MT nucleation activity did not contribute to the observed spindle shortening (see Chapter 3), we evaluated the role of known TPX2-interacting proteins Xklp2, Aurora A and Eg5 (Wittmann *et al.*, 2000; Bayliss *et al.*, 2003; Eckerdt *et al.*, 2008). Minimal differences in localization of Xklp2 and the previously identified scaling factor p60 katanin were observed upon addition of TPX2 to *X. laevis* egg extracts, and the subtle effects of Xklp2 inhibition were similar to published observations (Figure 2.6A; Walczak et al., 1998). Addition of recombinant *X. laevis* TPX2 lacking the first 39 amino acids that bind and activate the mitotic kinase Aurora A did not affect TPX2's ability to decrease spindle length. In contrast, a deletion mutant lacking the C-terminal 35 amino acids responsible for Eg5 binding lost the spindle shrinking activity seen with full-length TPX2 (Figure 2.6B). Additionally, this mutant no longer localized to the spindle, consistent with studies of other C-terminal deletion mutants (Brunet *et al.*, 2004).

Figure 2.6

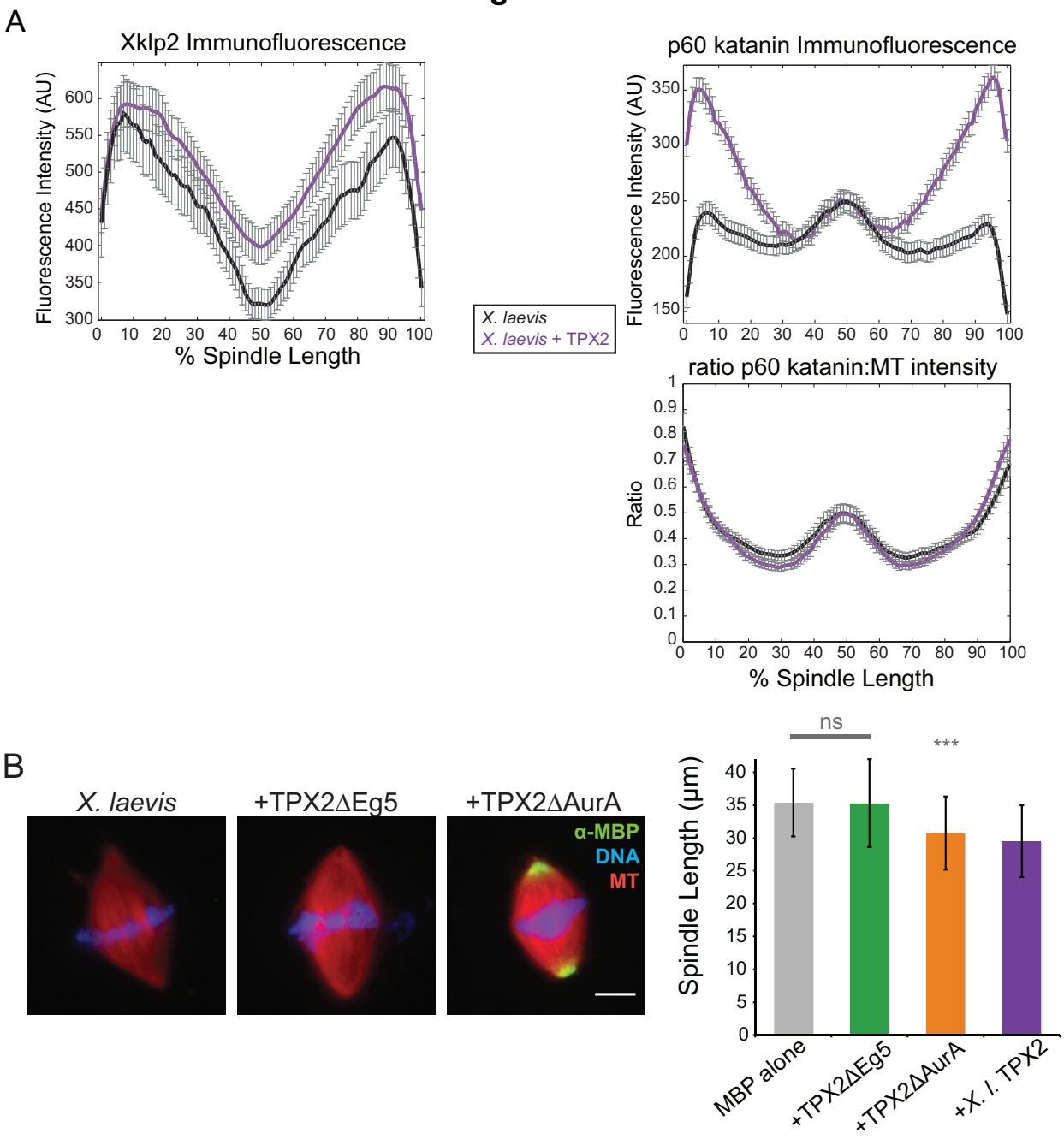
A
Xklp2 Immunofluorescence
Fluorescence Intensity (AU)
% Spindle Length
X. laevis
X. laevis + TPX2
p60 katanin Immunofluorescence
Fluorescence Intensity (AU)
ratio p60 katanin:MT intensity
Ratio
% Spindle Length
B
X. laevis
+TPX2ΔEg5
+TPX2ΔAurA
α-MBP
DNA
MT
ns
***
Spindle Length (µm)
MBP alone
+TPX2ΔEg5
+TPX2ΔAurA
+X. l. TPX2

Figure 2.6. TPX2 regulates spindle size through interaction with Eg5
(A) Line scan quantification of Xklp2 immunofluorescence or p60 katanin intensity in *X. laevis* spindles with and without addition of recombinant TPX2 to 200 nM. Spindle lengths were normalized for statistical analysis. Mean ± SE, n ≥ 90 spindles for each condition from three extracts for p60 staining, and n ≥ 42 spindles for each condition from two extracts for Xklp2 staining.. While p60 katanin localization increases slightly at the poles, comparing the katanin signal to MT intensity shows that the ratio of p60:MT remains unchanged. Xklp2 staining is not altered with TPX2 addition.

(B) Addition of TPX2 domain truncation mutants to *X. laevis* extract. The TPX2ΔAurA mutant localized like full-length TPX2 and had similar effects on spindle size, while TPX2ΔEg5 did not localize to the spindle or cause a decrease in spindle length. Scale bar is 10 μm. Mean ± SD, n ≥ 166 spindles in each condition from three separate extracts. ΔEg5 TPX2 mean is not significantly different from MBP control, but is significantly different from full-length TPX2 by unpaired t-test, $p<0.0001$.

To understand how the TPX2-Eg5 interaction contributes to spindle size, we looked for differences in Eg5 between the two *Xenopus* species. While concentrations of Eg5 were similar in the two egg extracts (Figure 2.4A), immunofluorescence staining revealed increased localization of Eg5 to spindle poles in *X. tropicalis* (Figure 2.7, A and B). Furthermore, addition of recombinant TPX2 to *X. laevis* increased the localization of Eg5 at spindle poles to similar levels. This relocalization activity was specific, as recombinant TPX2 lacking the Eg5 interaction domain did not alter Eg5 staining. Eg5 localization, therefore, can be regulated by TPX2 in a concentration-dependent manner. Concomitant with Eg5 localization changes, TPX2 addition caused a redistribution of MT density toward the poles (Figure 2.7, C and D), resulting in a spindle architecture with decreased MT density in the spindle center more like that of *X. tropicalis*.

It has been shown previously that TPX2 inhibits Eg5 motor activity *in vitro* (Ma et al., 2011). To test whether the added TPX2 mimicked Eg5 inhibition, we compared spindle morphology upon addition of 50 μM monastrol. Eg5 inhibition shortened *X. laevis* spindles, but a similar MT density across the spindle midzone was maintained, unlike the effects of TPX2 (Figure 2.7D). Although it is possible that the additional TPX2 also inhibits Eg5 motility, our results suggest that higher levels of TPX2 operate primarily by increasing the amount of Eg5 at the poles. An increase in polar Eg5 did not result from monastrol addition, or from other treatments that decreased spindle length, including addition of nocodozole or Op18 (Figure 2.7E). Thus, TPX2 specifically alters MT organization, and this in turn likely contributes to differences in meiotic spindle size between *X. laevis* and *X. tropicalis* (Figure 2.8).

Figure 2.7

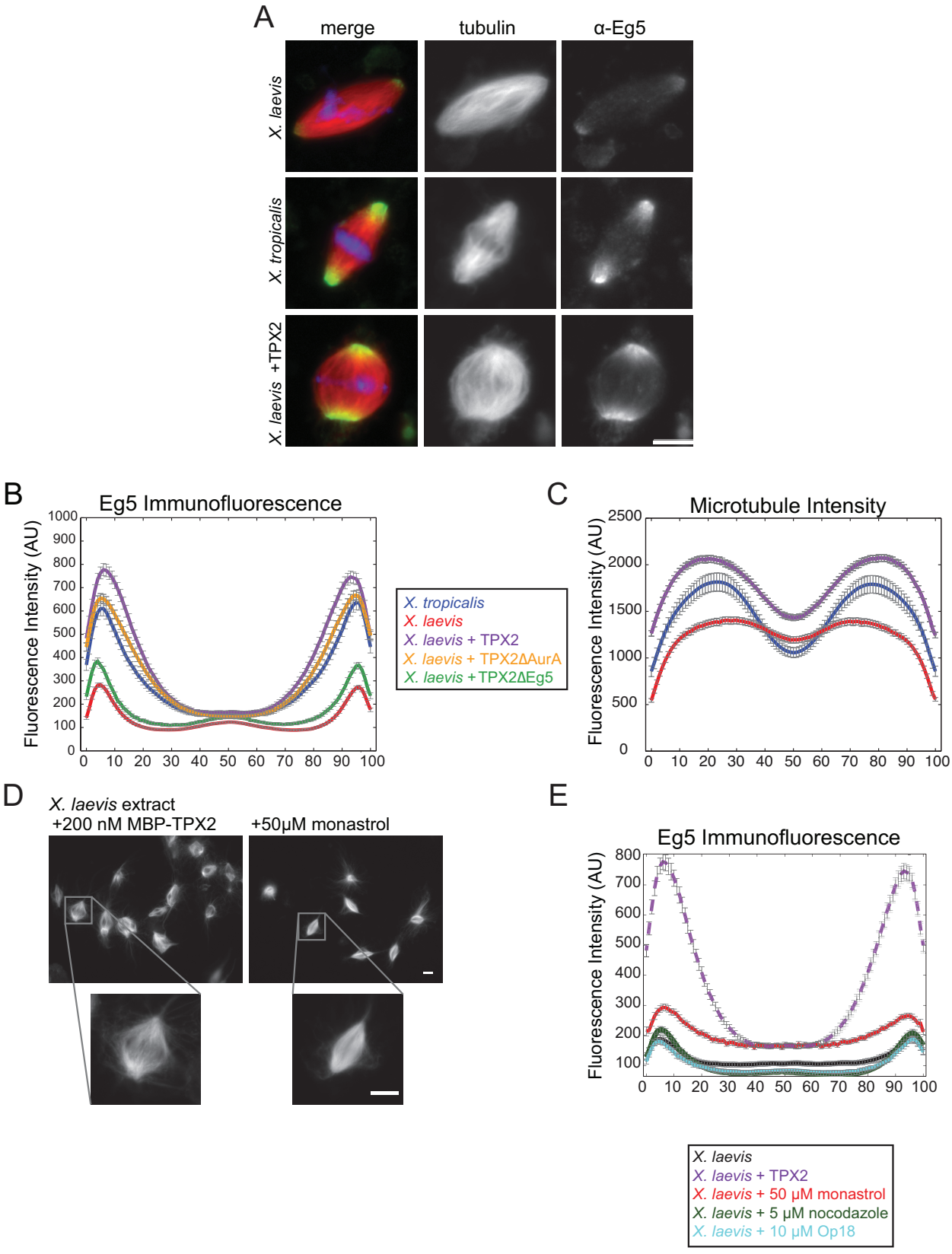
A
merge
tubulin
α-Eg5
X. laevis
X. tropicalis
X. laevis +TPX2
B
Eg5 Immunofluorescence
Fluorescence Intensity (AU)
X. tropicalis
X. laevis
X. laevis + TPX2
X. laevis + TPX2ΔAurA
X. laevis + TPX2ΔEg5
C
Microtubule Intensity
Fluorescence Intensity (AU)
D
X. laevis extract
+200 nM MBP-TPX2
+50μM monastrol
E
Eg5 Immunofluorescence
Fluorescence Intensity (AU)
X. laevis
X. laevis + TPX2
X. laevis + 50 μM monastrol
X. laevis + 5 μM nocodazole
X. laevis + 10 μM Op18

Figure 2.7 TPX2 regulates MT distribution through interaction with Eg5
(A) Representative images of Eg5 localization and MT density changes in *X. laevis* spindles upon addition of 200 nM MBP-TPX2. Left panels are merged, center panels show rhodamine-tubulin, and right panels show Eg5 immunofluorescence. Scale bar 10 μm.

(B) Line scan quantification of Eg5 immunofluorescence intensity in *X. tropicalis* and *X. laevis* spindles with and without addition of TPX2 mutants. Spindle lengths were normalized for statistical analysis. Mean ± SE, n ≥ 169 spindles for each condition from three extracts.

(C) Line scan quantification of MT density measured by rhodamine tubulin intensity in *X. tropicalis* and *X. laevis* spindles with and without addition of TPX2. Spindle lengths were normalized for statistical analysis. Mean ± SE, n ≥ 156 spindles for each condition from three extracts.

(D) Field of view images of *X. laevis* extract spindles with addition of 200 nM recombinant MBP-TPX2 or 50 μM monastrol. Insets highlight that while spindle size is similarly reduced in both cases, the MT distribution of each phenotype is distinct. Scale bars 10 μm.

(E) Line scan quantification of Eg5 immunofluorescence intensity after treatment with 10 μM Op18, 5 μM nocodazole, or 50 μM monastrol. Nocodazole and Op18, which both reduce spindle size, result in little change in Eg5 localization. Monastrol, which inhibits Eg5 motor activity, increases staining along the length of the entire spindle. Comparison to *X. laevis* + TPX2 data from panel B in purple, which shows significant polar recruitment of Eg5 to the spindle. Mean ± SE, n ≥ 60 spindles for each condition from two extracts.

Discussion

By comparing *X. laevis and X. tropicalis* meiotic spindles formed in egg extracts, we identified TPX2 as a factor whose levels contribute to fundamental spindle properties including assembly pathway, MT organization, and size. Since both species' spindles are the same type and perform the same function, we hypothesize that their differences reveal architectural features that distinguish small and large spindles (Figure 2.8).

A striking effect of higher TPX2 levels found in *X. tropicalis* egg extracts is loss of the requirement for RanGTP for spindle assembly. One possible explanation for this result is that at higher concentrations, TPX2 supports spindle formation in the absence of other Ran-regulated cargos. We favor an alternative mechanism, that excess TPX2 sequesters importin α through its atypical tight binding (Giesecke and Stewart, 2010), which could act to free other cargoes that induce MT nucleation and spindle assembly. Furthermore, importin α levels are reduced in *X. tropicalis* egg extracts compared to *X. laevis* (Levy and Heald, 2010), which could amplify this effect. We showed previously that importin α partitions from the cytoplasm to a membrane fraction during early *X. laevis* development, leading to greater spindle association of the kinesin-13 MT depolymerase Kif2a and spindle shrinkage by Stage 8 (Wilbur and Heald, 2013). Reduced cytoplasmic importin α in smaller cells may also contribute to the observed decrease in dependence on the Ran pathway, and other effects that transform spindle architecture during development.

Our results indicate that the major effect of TPX2 levels in modulating meiotic spindle size is by altering the distribution of the tetrameric kinesin-5 motor Eg5, which in turn shifts MT density from antiparallel overlap in the center of the spindle to the poles (Figure 2.8). In mammalian systems, mEg5 localization has been shown to be highly dynamic during mitosis, as TPX2 translocates mEg5 toward the minus-ends of MTs through its association with dynein (Gable *et al.*, 2012). Our data indicate that increased TPX2 levels stimulate this movement, which shifts Eg5 activity from the center of the spindle, where it slides antiparallel MTs apart minus-end out, to the poles where MTs are of more uniform polarity, thereby converting its activity to MT crosslinking. We wondered whether poleward MT flux rates, which depend on Eg5 antiparallel sliding, would be altered (Miyamoto *et al.*, 2004). Due to extract-to-extract variability in flux measurements (Miyamoto *et al.*, 2004) and technical challenges of live imaging in *X. tropicalis*, we were unable to identify TPX2-dependent changes in flux, though previous measurements of *X. laevis* and *X. tropicalis* rates were not significantly different (Brown *et al.*, 2007). Since an increase in Eg5 localization at the poles might not reduce its activity on antiparallel MTs, it is possible that flux would still occur with only subtle changes.

Figure 2.8

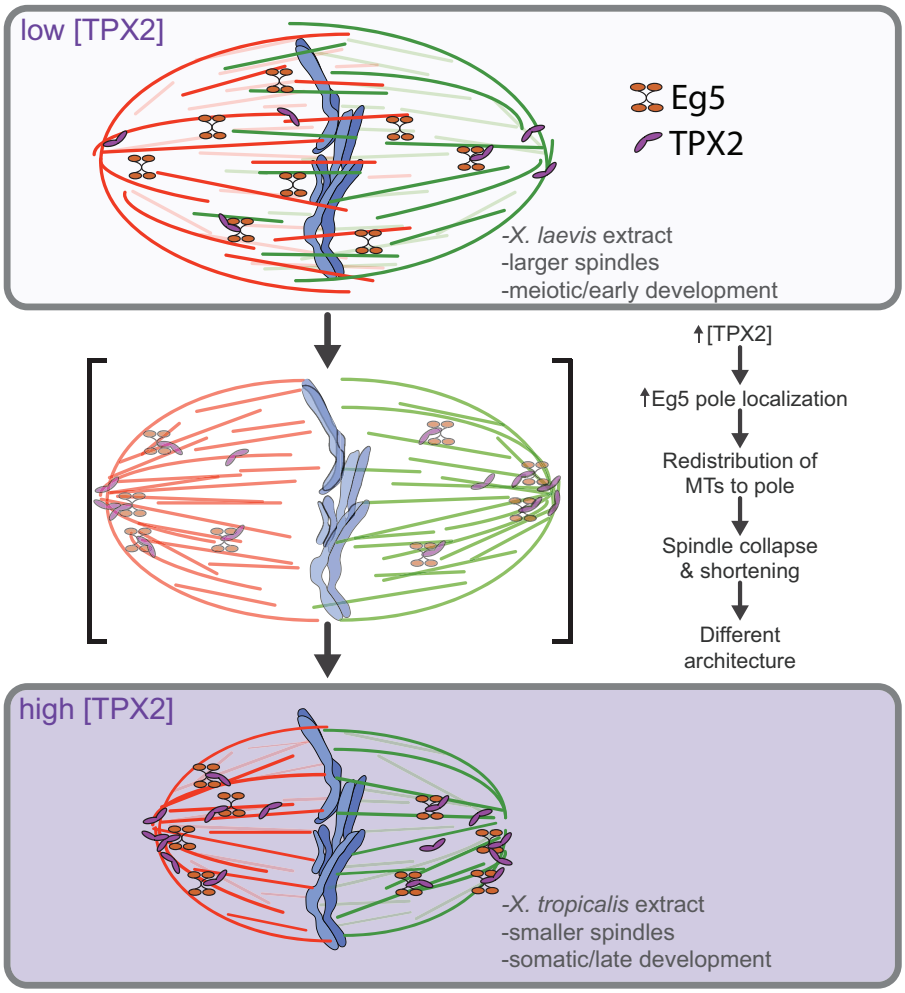

Figure 2.8 Model of TPX2 regulation of spindle size and MT distribution via Eg5
MTs with plus-ends to the right are labeled in red while MTs with the opposite orientation are labeled in green. An increase in TPX2 (purple) concentration would recruit more Eg5 (orange) to the spindle poles, reducing the extent of antiparallel MT overlap and increasing MT crosslinking at spindle poles. Reduced antiparallel MT cross-linking in the midzone array causes spindle length to decrease.

While TPX2 has been well-studied in many systems for its role in spindle assembly, it is interesting to note that it is not well-conserved across phylogenies, and precise TPX2 functions appear to correlate with the presence or absence of certain domains (Goshima, 2011; Helmke *et al.*, 2013). In contrast to the activity of TPX2 to decrease spindle length described here for *Xenopus*, increased amounts of the *C. elegans* TPX2-like protein (TPXL) correlated with increased spindle size (Greenan *et al.*, 2010). However, the *C. elegans* ortholog differs in that it lacks the C-terminal Eg5 binding domain and only contains the conserved Aurora A-binding region at the N-terminus of the protein, a region which is dispensable for function in *Xenopus* (Brunet *et al.*, 2004; Karsenti, 2005). In *Drosophila* S2 cells, the TPX2-like protein D-TPX2 contains neither the Aurora A- or Eg5- binding domains, and is dispensable for cell division, although its depletion resulted in a short spindle phenotype (Goshima *et al.*, 2007). In humans and *Xenopus,* the interaction of TPX2 with Eg5 appears to be crucial for modulating spindle integrity, size, and localization (Brunet *et al.*, 2004; Ma *et al.*, 2010; 2011; Gable *et al.*, 2012). We speculate that TPX2 has evolved to help specify unique spindle architectures in different systems.

The changes in Eg5 and RanGTP dependency we describe here have also been observed in early embryo development of other species, when spindles become smaller due to rapid reductive divisions of the zygote. In mouse embryos, the first three cleavages require kinesin-5 activity, but thereafter, spindle bipolarity is kinesin-5 independent (Fitzharris, 2009). It has also been observed that in some mammalian somatic systems, with spindles roughly half the length as in *Xenopus* meiotic systems (~10-15 μm), the requirements of Ran and Eg5 are also decreased (Kapoor *et al.*, 2000; Kalab *et al.*, 2006; Vanneste *et al.*, 2009; Wilbur and Heald, 2013). Taken together, our results have implications for general differences in MT architecture between small and large spindles. Large spindles, required for separating chromosomes over relatively large distances in eggs and early embryos, depend on MT generation at the spindle midzone through RanGTP induced nucleation and organization by kinesin-5 activity. In *Xenopus* at least, assembly of smaller spindles spanning shorter distances appears to be directed by centrosomes and contain a higher proportion of k-fibers relative to spindle MTs that are instrumental in spindle stability (Loughlin et al., 2011; Wilbur and Heald, 2013).

Ultimately, we do not yet know the crucial details of spindle architecture, such as the organization of MT bundles and the location of MT plus and minus ends. Advances in electron tomography and high resolution imaging that overcome the challenge of high MT density in the spindle will enable detailed comparisons, which combined with molecular perturbation, will elucidate the basis of distinct spindle architectures and its importance for spindle function in different cell types.

Materials and Methods

Xenopus egg extracts and spindle assembly reactions

X. laevis and *X. tropicalis* egg extracts were prepared and induced to progress through the cell cycle as described (Maresca and Heald, 2006; Brown et al., 2007; Hannak and Heald, 2006). Demembranated *X. laevis* sperm nuclei (to final concentration of 15000 nuclei/µl) were added to CSF extract and released into interphase by the addition of 0.5 mM CaCl2. After approximately 1 hour, nuclei that had decondensed and replicated were flash frozen in extract with 8% glycerol and stored at -80^{o}C. To assemble metaphase spindles, replicated nuclei were resuspended in Egg Lysis Buffer (250 mM sucrose, 50 mM KCl, 2.5 mM MgCl2, 10 mM HEPES pH 7.8) and pelleted by centrifugation at 1600xg for 5 minutes at room temperature. Nuclei were then resuspended in CSF extracts (500 nuclei/µl) and incubated at room temperature for 30-45 minutes while spindle formation occurred. Spindles were visualized by supplementing the extract with X-rhodamine–labeled tubulin (50 µg/ml). For experiments with recombinant protein or inhibitors, all components were added prior to spindle assembly. Where noted, spindle reactions were preserved by fixation with Spindle Fixative (48% glycerol, 1X MMR, 11% formaldehyde, 5 µg/ml Hoechst, (Maresca and Heald, 2006)) under coverglass.

Immunofluorescence analysis

Immunofluorescence staining of fixed spindles was performed according to (Maresca and Heald, 2006). The rabbit antibody to TPX2 raised against 100 N-terminal a.a. was produced by Strategic Diagnostics Inc (SDIX) and used 1:3000. Anti-MBP monoclonal mouse antibody from New England Biolabs (E8030S), was used 1:2000. Rabbit antibodies raised to Eg5-stalk domain and Xklp2 were kind gifts from Claire Walczak and used at 1:400 (Sawin et al., 1992; Walczak et al., 1998). Spindles in extract were fixed with 3.7% formaldehyde, sedimented through a 40% glycerol cushion onto coverslips, post fixed in 100% methanol and blocked with PBS-1% BSA. Coverslips were incubated with primary antibody, washed extensively with PBS-0.1% NP-40 and incubated with a 1:1000 dilution of secondary antibody (Alexa 488 labeled anti-rabbit or anti-mouse, Invitrogen).

Images were obtained on an Olympus BX51 fluorescence microscope with TRITC, DAPI, and FITC filters (Chroma Technology) and a 40x objective (UPlanFl N, Olympus; NA 0.75) controlled by µManager (http://www.micro-manager. org/) with a Hamamatsu Orca-ER cooled CCD camera. Immunofluorescence analysis was performed as previously described (Loughlin et al., 2011; Wilbur and Heald, 2013). Briefly, for widefield fluorescence, 20-pixel-width linescans were manually taken in ImageJ along the long axis of the spindle on background-subtracted images. For spinning disk confocal images, 50-pixel-width linescans were taken on background-subtracted images. Data was then normalized to 100% spindle length, and intensity was averaged within each 1% length bin. Depending on the length of the spindle, ~2 to 6 pixels were averaged per length bin. Spindles from each condition were averaged under these normalized spindle length conditions with error propagation and intensity plotted as a function of 0–100% spindle length. Spindle length was quantified using MATLAB as previously described (Loughlin et al., 2011).

Spinning disk confocal imaging

Confocal slices were taken on a Nikon Spinning Disk confocal microscope (Andor Technologies) with 561nm and 404nm lasers and a 100x objective (Nikon Plan Apo 100x; 1.45 N.A.) controlled by MetaMorph on an Andor iXon3 EMCCD camera.

Western blotting

Primary antibodies described above were used at the same dilutions for Western blot as for immunofluorescence in PBST-5% Milk. Primary antibody to beta-tubulin (mouse anti-tubulin, Developmental Studies Hybridoma Bank, E7) was used 1:5000. Secondary antibodies were obtained from Rockland Immunochemicals (goat anti-rabbit IRDye 800 or goat anti-mouse IRDye 700) and used 1:10000. Blots were scanned with an Odyssey Infrared Imaging System (LI-COR Biosciences) and band intensity quantified with the LI-COR software.

Protein purification

RanT24N, RanQ69L, and importin beta (71-876) were purified as previously described (Weis et al., 1996; Chi et al., 1997). *X. tropicalis* and *X. laevis* cDNA for TPX2 were obtained from Open Biosystems and cloned into pMAL-c5x (New England Biolabs) with an additional 6x His tag added c-terminally to the coding sequence (named pMBP-TPX2). Proteins were expressed overnight at room temperature with 1 mM IPTG and two-step affinity purified first with NiNTA agarose (Sigma) followed by binding to amylose resin (New England Biolabs) in 25 mM HEPES pH 7.7, 250 mM NaCl or KCl, 2 mM MgCl2, and 50 mM sucrose. pMBP-Laevis TPX2 Δ7 was generated by site-directed mutagenesis to remove the amino acids 619-(LSGSIVQ)-625, and pMBP- Laevis TPX2 3SA mutant was changed to alter the proximal serines to alanine 618-ALAGAIVQ-625. pMBP- Trop TPX2 +7 was generated by site-directed mutagenesis to insert the amino acids found in *X. laevis* into the homologous region of the *X. tropicalis* protein: 619T-LSGSIVQ-E620. pMBP-L TPX2 ΔAurA was truncated to remove the n-terminal first 39 amino acids of the protein, and pMBP-L TPX2 ΔEg5 was truncated to remove the last c-terminal 35 amino acids (Bayliss et al., 2003; Eckerdt et al., 2008).

References

Bayliss, R., Sardon, T., Vernos, I., and Conti, E. (2003). Structural basis of Aurora-A activation by TPX2 at the mitotic spindle. Mol Cell *12*, 851–862.

Bird, A. W., and Hyman, A. A. (2008). Building a spindle of the correct length in human cells requires the interaction between TPX2 and Aurora A. J Cell Biol *182*, 289–300.

Brown, K. S., Blower, M. D., Maresca, T. J., Grammer, T. C., Harland, R. M., and Heald, R. (2007). Xenopus tropicalis egg extracts provide insight into scaling of the mitotic spindle. J Cell Biol *176*, 765–770.

Brugués, J., Nuzzo, V., Mazur, E., and Needleman, D. J. (2012). Nucleation and transport organize microtubules in metaphase spindles. Cell *149*, 554–564.

Brunet, S., Sardon, T., Zimmerman, T., Wittmann, T., Pepperkok, R., Karsenti, E., and Vernos, I. (2004). Characterization of the TPX2 Domains Involved in Microtubule Nucleation and Spindle Assembly in Xenopus Egg Extracts. Mol. Biol. Cell *15*, 5318–5328.

Carazo-Salas, R. E., Guarguaglini, G., Gruss, O. J., Segref, A., Karsenti, E., and Mattaj, I. W. (1999). Generation of GTP-bound Ran by RCC1 is required for chromatin-induced mitotic spindle formation. Nature *400*, 178–181.

Chi, N. C., Adam, E. J., and Adam, S. A. (1997). Different binding domains for Ran-GTP and Ran-GDP/RanBP1 on nuclear import factor p97. J Biol Chem *272*, 6818–6822.

Cole, D. G., Saxton, W. M., Sheehan, K. B., and Scholey, J. M. (1994). A “slow” homotetrameric kinesin-related motor protein purified from Drosophila embryos. J Biol Chem *269*, 22913–22916.

Eckerdt, F., Eyers, P. A., Lewellyn, A. L., Prigent, C., and Maller, J. L. (2008). Spindle pole regulation by a discrete Eg5-interacting domain in TPX2. Curr Biol *18*, 519–525.

Fitzharris, G. (2009). A shift from kinesin 5-dependent metaphase spindle function during preimplantation development in mouse. Development *136*, 2111–2119.

Gable, A. *et al.* (2012). Dynamic reorganization of Eg5 in the mammalian spindle throughout mitosis requires dynein and TPX2. Mol. Biol. Cell *23*, 1254–1266.

Giesecke, A., and Stewart, M. (2010). Novel Binding of the Mitotic Regulator TPX2 (Target Protein for Xenopus Kinesin-like Protein 2) to Importin. Journal of Biological Chemistry *285*, 17628–17635.

Goshima, G. (2011). Identification of a TPX2-like microtubule-associated protein in Drosophila. PLoS ONE *6*, e28120.

Goshima, G., Wollman, R., Goodwin, S. S., Zhang, N., Scholey, J. M., Vale, R. D., and Stuurman, N. (2007). Genes required for mitotic spindle assembly in Drosophila S2

cells. Science *316*, 417–421.

Goshima, G., Wollman, R., Stuurman, N., Scholey, J. M., and Vale, R. D. (2005). Length control of the metaphase spindle. Curr Biol *15*, 1979–1988.

Greenan, G., Brangwynne, C. P., Jaensch, S., Gharakhani, J., Jülicher, F., and Hyman, A. A. (2010). Centrosome size sets mitotic spindle length in Caenorhabditis elegans embryos. Curr Biol *20*, 353–358.

Gruss, O. J., Carazo-Salas, R. E., Schatz, C. A., Guarguaglini, G., Kast, J., Wilm, M., Le Bot, N., Vernos, I., Karsenti, E., and Mattaj, I. W. (2001). Ran induces spindle assembly by reversing the inhibitory effect of importin alpha on TPX2 activity. Cell *104*, 83–93.

Hannak, E., and Heald, R. (2006). Investigating mitotic spindle assembly and function in vitro using Xenopus laevis egg extracts. Nat Protoc *1*, 2305–2314.

Helmke, K. J., Heald, R., and Wilbur, J. D. (2013). Interplay between spindle architecture and function. Int Rev Cell Mol Biol *306*, 83–125.

Kalab, P., Pralle, A., Isacoff, E. Y., Heald, R., and Weis, K. (2006). Analysis of a RanGTP-regulated gradient in mitotic somatic cells. Nat Cell Biol *440*, 697–701.

Kalab, P., Pu, R. T., and Dasso, M. (1999). The ran GTPase regulates mitotic spindle assembly. Curr Biol *9*, 481–484.

Kalab, P., Weis, K., and Heald, R. (2002). Visualization of a Ran-GTP Gradient in Interphase and Mitotic Xenopus Egg Extracts. Science *295*, 2452–2456.

Kapoor, T. M., Mayer, T. U., Coughlin, M. L., and Mitchison, T. J. (2000). Probing spindle assembly mechanisms with monastrol, a small molecule inhibitor of the mitotic kinesin, Eg5. J Cell Biol *150*, 975–988.

Karsenti, E. (2005). TPX or Not TPX? Mol Cell *19*, 431–432.

Levy, D. L., and Heald, R. (2010). Nuclear Size Is Regulated by Importin α and Ntf2 in Xenopus. Cell *143*, 288–298.

Loughlin, R., Heald, R., and Nédélec, F. (2010). A computational model predicts Xenopus meiotic spindle organization. J Cell Biol *191*, 1239–1249.

Loughlin, R., Wilbur, J. D., McNally, F. J., Nédélec, F. J., and Heald, R. (2011). Katanin Contributes to Interspecies Spindle Length Scaling in Xenopus. Cell *147*, 1397–1407.

Ma, N., Titus, J., Gable, A., Ross, J. L., and Wadsworth, P. (2011). TPX2 regulates the localization and activity of Eg5 in the mammalian mitotic spindle. J Cell Biol *195*, 87–98.

Ma, N., Tulu, U. S., Ferenz, N. P., Fagerstrom, C., Wilde, A., and Wadsworth, P. (2010). Poleward transport of TPX2 in the mammalian mitotic spindle requires dynein, Eg5, and

microtubule flux. Mol. Biol. Cell *21*, 979–988.

Maliga, Z., and Mitchison, T. J. (2006). Small-molecule and mutational analysis of allosteric Eg5 inhibition by monastrol. BMC Chem Biol *6*, 2.

Maresca, T. J., and Heald, R. (2006). Methods for studying spindle assembly and chromosome condensation in Xenopus egg extracts. Methods Mol. Biol. *322*, 459–474.

Miyamoto, D. T., Perlman, Z. E., Burbank, K. S., Groen, A. C., and Mitchison, T. J. (2004). The kinesin Eg5 drives poleward microtubule flux in Xenopus laevis egg extract spindles. J Cell Biol *167*, 813–818.

Nachury, M. V., Maresca, T. J., Salmon, W. C., Waterman-Storer, C. M., Heald, R., and Weis, K. (2001). Importin beta is a mitotic target of the small GTPase Ran in spindle assembly. Cell *104*, 95–106.

Needleman, D. J., Groen, A., Ohi, R., Maresca, T., Mirny, L., and Mitchison, T. (2010). Fast microtubule dynamics in meiotic spindles measured by single molecule imaging: evidence that the spindle environment does not stabilize microtubules. Mol. Biol. Cell *21*, 323–333.

Ohba, T., Nakamura, M., Nishitani, H., and Nishimoto, T. (1999). Self-organization of microtubule asters induced in Xenopus egg extracts by GTP-bound Ran. Science *284*, 1356–1358.

Sawin, K. E., LeGuellec, K., Philippe, M., and Mitchison, T. J. (1992). Mitotic spindle organization by a plus-end-directed microtubule motor. Nature *359*, 540–543.

Schatz, C. A., Santarella, R., Hoenger, A., Karsenti, E., Mattaj, I. W., Gruss, O. J., and Carazo-Salas, R. E. (2003). Importin alpha-regulated nucleation of microtubules by TPX2. Embo J *22*, 2060–2070.

van den Wildenberg, S. M. J. L., Tao, L., Kapitein, L. C., Schmidt, C. F., Scholey, J. M., and Peterman, E. J. G. (2008). The homotetrameric kinesin-5 KLP61F preferentially crosslinks microtubules into antiparallel orientations. Curr Biol *18*, 1860–1864.

Vanneste, D., Takagi, M., Imamoto, N., and Vernos, I. (2009). The Role of Hklp2 in the Stabilization and Maintenance of Spindle Bipolarity. Current Biology *19*, 1712–1717.

Walczak, C. E., Vernos, I., Mitchison, T. J., Karsenti, E., and Heald, R. (1998). A model for the proposed roles of different microtubule-based motor proteins in establishing spindle bipolarity. Curr Biol *8*, 903–913.

Weis, K., Dingwall, C., and Lamond, A. I. (1996). Characterization of the nuclear protein import mechanism using Ran mutants with altered nucleotide binding specificities. Embo J *15*, 7120–7128.

Wilbur, J. D., and Heald, R. (2013). Mitotic spindle scaling during Xenopus development

by kif2a and importin α. Elife *2*, e00290.

Wilde, A., and Zheng, Y. (1999). Stimulation of microtubule aster formation and spindle assembly by the small GTPase Ran. Science *284*, 1359–1362.

Wittmann, T., Wilm, M., Karsenti, E., and Vernos, I. (2000). TPX2, A novel xenopus MAP involved in spindle pole organization. J Cell Biol *149*, 1405–1418.

Yang, G., Cameron, L. A., Maddox, P. S., Salmon, E. D., and Danuser, G. (2008). Regional variation of microtubule flux reveals microtubule organization in the metaphase meiotic spindle. J Cell Biol *182*, 631–639.

Zhang, C., Hughes, M., and Clarke, P. R. (1999). Ran-GTP stabilises microtubule asters and inhibits nuclear assembly in Xenopus egg extracts. J Cell Sci *112 (Pt 14)*, 2453–2461.

Chapter 3: Microtubule Nucleation by TPX2 is Regulated by a Short C-terminal Region and Regulates Spindle Pole Morphology

Background

Unlike the other major cytoskeletal component, actin, the mechanics of MT nucleation have not been well-described. The only known nucleator is the γ-tubulin ring complex (γ-TuRC) whose crystal structure suggests that it templates the growth of a MT by stabilizing and capping from the minus-end (Hannak *et al.*, 2002; Kollman *et al.*, 2010; Guillet *et al.*, 2011; Kollman *et al.*, 2011). While we know that augmin contributes to nucleation, it appears this is also mediated by γ-tubulin (Uehara *et al.*, 2009).

Immunodepletion of TPX2 completely abrogated RanGTP-dependent MT nucleation in *Xenopus* egg extracts, and recombinant TPX2 could induce MT nucleation in solutions of pure tubulin *in vitro,* but the mechanism of its action in MT nucleation is unclear (Gruss et al., 2001; Schatz et al., 2003). This protein is predicted to have little tertiary structure and may oligomerize, but it remains unclear whether TPX2 nucleates MTs directly or if it acts to stabilize small MT assemblies or requires other cellular factors such as the γ-TuRC for activity. Studies investigating the protein complex Augmin demonstrated an important role for TPX2 in organization of MTs during nucleation. Addition of excess Ran and TPX2 to *Xenopus* egg extracts induced the formation of MT aster structures called “fans” which maintain minus-ends at a single point (Petry et al., 2013). Fan formation and robust nucleation required the activity of γ-tubulin, Augmin, and TPX2, suggesting all might cooperate in MT nucleation (Figure 1.2). This activity was also shown to reside in the c-terminal half of TPX2, and this dissertation expands upon the nucleation capacity of TPX2.

Taking advantage of the comparisons between species orthologs of TPX2 from *X. tropicalis* and *X. laevis,* we show here inherent species differences in the nucleation capacity of this protein. Sequence alignments show a small 7 amino acid deletion in the *X. tropicalis* protein that correlates with higher nucleation activity, which we have characterized with mutational analysis. Altering nucleation in this way contributed to pole morphology of the spindle by inducing astral MT projections, but ultimately did not affect spindle length.

Results

MT nucleation activity of *X. tropicalis* and *X. laevis* TPX2 differ in kinetics

In addition to concentration effects of TPX2 in spindle morphology determination, we wondered whether differences in TPX2 protein sequence, which is 76% identical and 87% conserved between the two *Xenopus* species, also contributed to differences in its activity (Figure 3.2A). We therefore purified recombinant versions of both *X. tropicalis* and *X. laevis* TPX2 and added them to *X. laevis* extract, and observed that *X. tropicalis* TPX2 possessed much higher MT nucleation activity. Imaging with TIRF microscopy revealed increased kinetics of nucleation, and while *X. laevis* TPX2 induced long and long-lived MTs, the *X. tropicalis* ortholog induced many short MTs (Figure 3.1).

At steady-state, the number of MT asters formed per field was approximately four-fold higher, and increased MT formation was observed at spindle poles in the presence of *X. tropicalis* TPX2, as astral arrays formed that were not observed in control spindles, or in spindles to which the same concentration of *X. laevis* TPX2 had been added (Figure 3.2, B and C). When added to *X. tropicalis* egg extracts, increased MT nucleation was less apparent (data not shown), presumably because the higher MT severing activity of *X. tropicalis* katanin trims astral MTs (Loughlin et al., 2011).

Figure 3.1

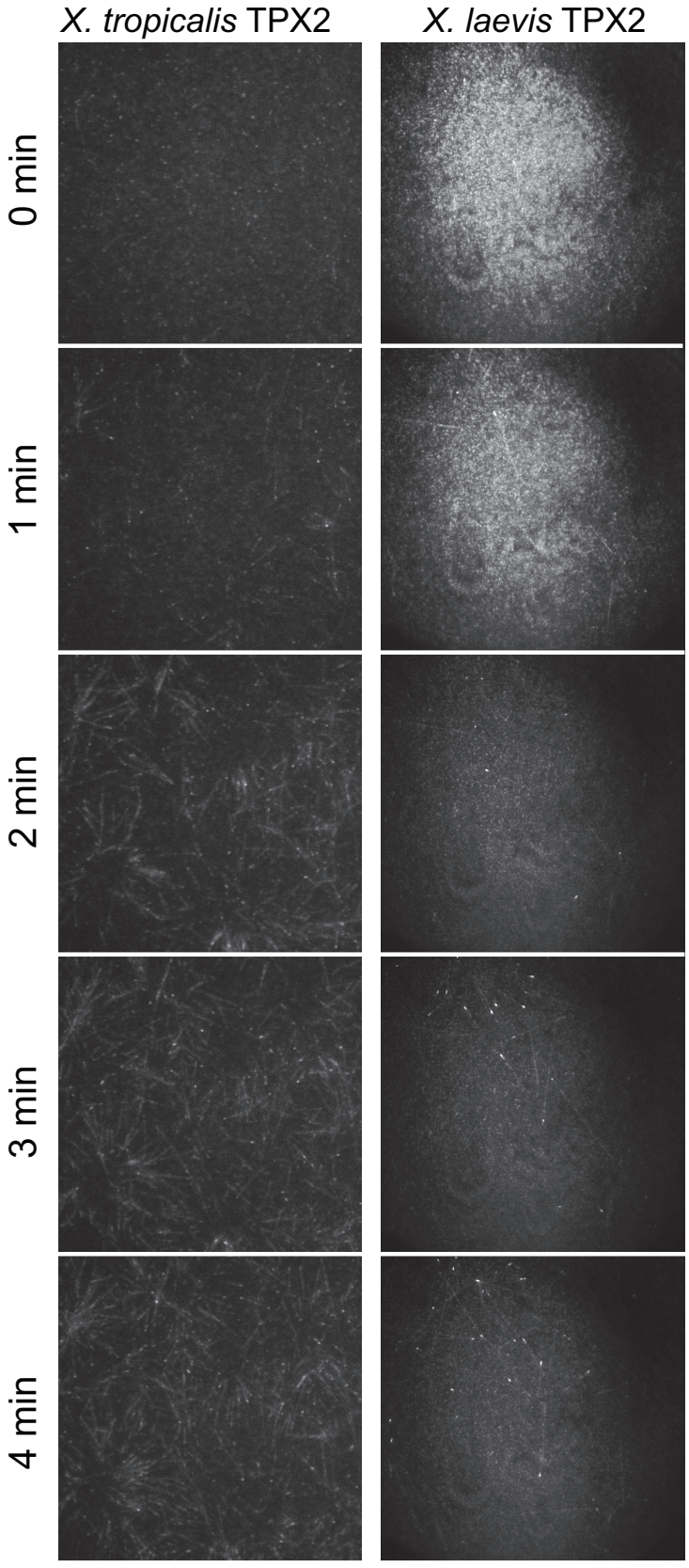

Figure 3.1 *X. tropicalis* and *X. laevis* orthologs of TPX2 have different MT nucleation kinetics and morphology in *X. laevis* extract
Time course images of recombinant *X. tropicalis* MBP-TPX2 and *X. laevis* MBP-TPX2 added to *X. laevis* extract visualized by TIRF microscopy. *X. tropicalis* TPX2 induces MT nucleation much earlier (starting at ~1 min compared to ~3 min for *X. laevis* TPX2) and with increased density. The MTs formed after *X. tropicalis* TPX2 addition, tracked with GFP-EB1 (bright foci), appear shorter and have quicker turnover than those from *X. laevis* TPX2. Images collected by S. Petry in the Vale lab at UCSF.

TPX2 nucleation activity is regulated by a 7 amino acid region

To investigate the disparity in TPX2-mediated MT nucleation between the two frog species, we scanned for primary sequence differences. Overall, the orthologs are 76% identical and 87% conserved with all verified Aurora A and Polo-like kinase 1 (Plx1) phosphorylation sites conserved (Eyers et al., 2003; Eckerdt et al., 2009). One difference that stood out was a 7 amino acid deletion in the *X. tropicalis* protein relative to *X. laevis* near the C-terminus, just upstream of the Eg5-binding domain (Figure 3.2A).

Remarkably, deletion of this sequence (amino acids 619-625) from recombinant *X. laevis* TPX2 increased its MT nucleation activity in *X. laevis* egg extract, while insertion of the sequence at the corresponding site in *X. tropicalis* TPX2 reduced its activity, suggesting that this 7 amino acid region is necessary and sufficient to modulate the nucleation activity of TPX2 (Figure 3.2, B and C). Absence of this same region in the TPX2 sequence also correlated with the formation of astral MT arrays at the poles of spindles formed in *X. laevis* extract (Figure 3.2B).

Figure 3.2

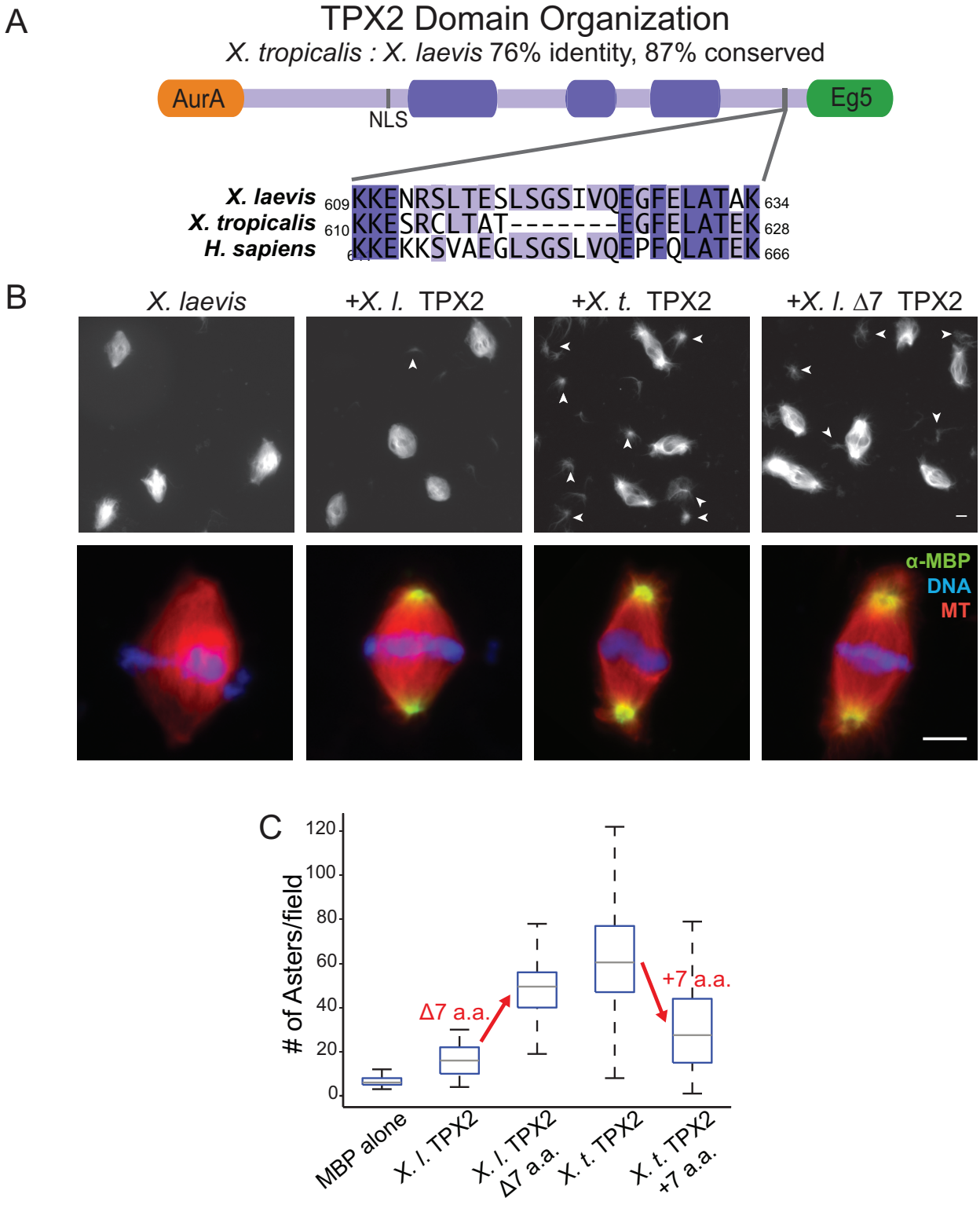
A
TPX2 Domain Organization
X. tropicalis : X. laevis 76% identity, 87% conserved
AurA
NLS
Eg5
X. laevis 609 KKENRSLTESLSGSIVQEGFELATAK 634
X. tropicalis 610 KKESRCLTAT-------EGFELATEK 628
H. sapiens KKEKKSVAEGLSGSLVQEPFQLATEK 666
B
X. laevis
+X. l. TPX2
+X. t. TPX2
+X. l. Δ7 TPX2
α-MBP
DNA
MT
C
# of Asters/field
0
20
40
60
80
100
120
Δ7 a.a.
+7 a.a.
MBP alone
X. l. TPX2
X. l. TPX2 Δ7 a.a.
X. t. TPX2
X. t. TPX2 +7 a.a.

Figure 3.2. TPX2 MT nucleation activity is regulated by a 7 amino acid sequence that contributes to spindle pole morphology
(A) Domain schematic of the *X. laevis* TPX2 protein. The first 39 amino acids are unstructured and interact with Aurora A (orange) and the last 35 amino acids interact with Eg5 (green) (Bayliss et al., 2003; Eckerdt et al., 2008). A mapped nuclear localization signal exists at a.a. 284. Three highly conserved domains are denoted by dark purple shading (Goshima, 2011). Zoom in shows conservation between *X. laevis* and human of a 7 amino acid sequence missing from the *X. tropicalis* ortholog.

(B) Addition of 200 nM recombinant TPX2 mutants to *X. laevis* extract. Top panels: 20x field of view showing increased MT aster structures nucleated upon addition of *X. tropicalis* TPX2 or *X. laevis* Δ7 TPX2 compared to control or *X. laevis* TPX2. White arrowheads indicate MT asters. Bottom panels: Spindle morphology after TPX2 mutant addition. *X. tropicalis* TPX2 and *X. laevis* Δ7 TPX2 induced formation of radial astral MTs emanating from the poles not seen in control spindles or with *X. laevis* TPX2 addition. Scale bars 10 μm.

(C) Quantification of nucleation activity of recombinant TPX2 proteins. For each condition, spindle reactions were sedimented onto coverslips as described in Materials and Methods and the number of MT aster structures was counted in 10 microscope fields, repeated in 3 separate extracts. Boxplot of # of asters per field with median marked by gray line, 1st and 3rd quartiles marked by box edges, and data maxima and minima noted by whiskers.

Phosphoregulation does not seem to contribute to nucleation activity

Interestingly, although the *X. laevis* serines 620 and 622 match the consensus site for phosphorylation by Plx1 (Nakajima et al., 2003), changing them and the adjacent Ser 618 to alanine in recombinant *X. laevis* TPX2 did not alter nucleation activity (Figure 3.3), indicating that phosphorylation of these sites, if it occurs, is not sufficient to account for the variation. Thus, a short amino acid sequence difference between *X. laevis* and *X. tropicalis* TPX2 regulates its MT nucleation activity, but the underlying mechanism requires further investigation.

Nucleation activity of TPX2 does not contribute to steady-state spindle size

These TPX2 mutants allowed us to test the effects of altering MT nucleation activity on spindle size. Although addition of TPX2 proteins that increased MT nucleation caused formation of astral MTs not usually present in *Xenopus* meiotic spindles (Figure 3.2B), pole-to-pole spindle length decreased regardless of TPX2 nucleation capacity (Figure 3.4). This result indicates that while TPX2 nucleation activity alters architecture at the pole, this mechanism of action is distinct from how TPX2 modulates steady-state spindle length.

Figure 3.3

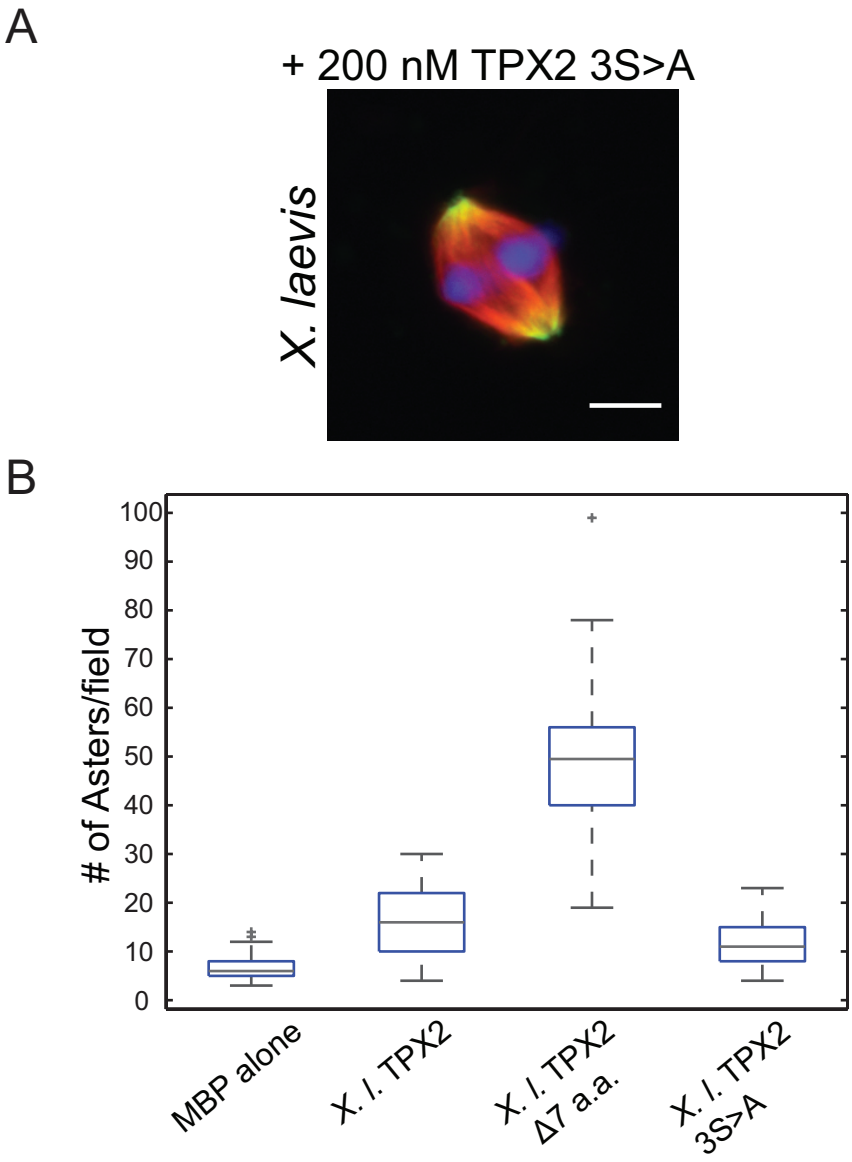

Figure 3.3. Phospho-null mutant of *X. laevis* TPX2 does not show altered MT nucleation activity

(A) Top panel shows spindle morphology upon addition of phospho-null mutant of *X. laevis* TPX2 (S218A, S220A, S222A) to *X. laevis* extract. Recombinant protein did not induce MT astral formation, similar to wildtype *X. laevis* TPX2. Scale bar 10 μm.

(B) Nucleation measured by asters per field (as described in Figure 3C, outliers indicated by "+") shows phospho-null mutant behaved like wildtype *X. laevis* TPX2 and not like the *X. laevis* Δ7 mutant.

Figure 3.4

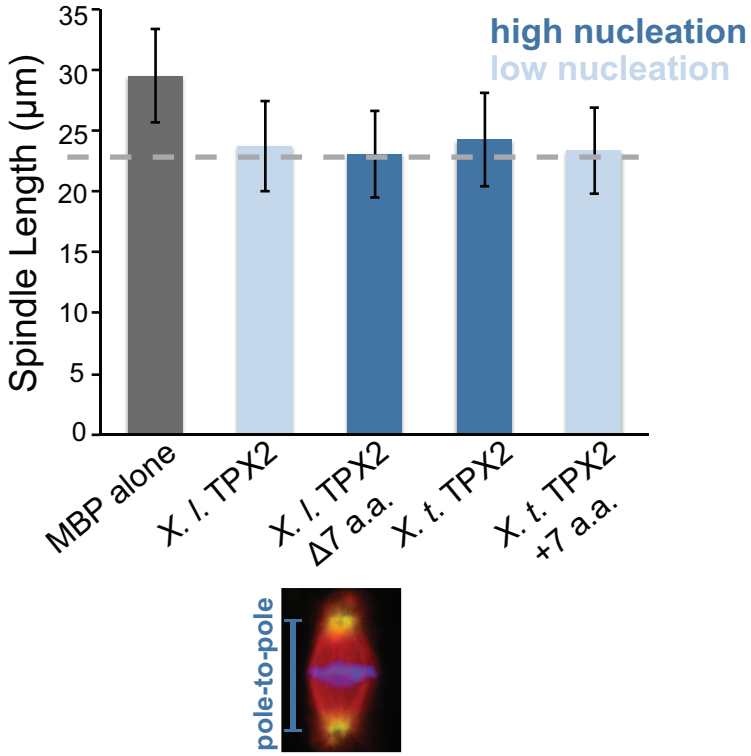

Figure 3.4 TPX2 MT nucleation activity is regulated by a 7 amino acid sequence that regulates spindle pole morphology, but not length
Quantification of pole-to-pole spindle length, not including astral MT projections, with addition of 200 nM MBP-TPX2 proteins compared to control of addition of 200 nM MBP. Mean ± SD, n ≥ 671 spindles in each condition from three separate extracts. For each TPX2 protein compared to MBP control, $p<0.0001$ from unpaired t-test.

Discussion

Understanding the exact architecture of the spindle is confounded by the high density of MTs, which ultimately may be understood by the advancement of super-resolution and electron microscopy. Because depletion of γ-tubulin severely disrupts spindle structure, it is difficult to discern the role of nucleation in setting spindle architecture. Furthermore, there has not been a method to specifically alter the positional nucleation of MTs within the spindle. This lack of knowledge about the contributions of nucleation in the spindle have precluded their inclusion in computational models of spindle architecture, making nucleation the “black box” of spindle morphology.

Here we show that nucleation activity can be modulated by TPX2, and a small 7 amino acid sequence in TPX2 is necessary and sufficient to attenuate its MT nucleation activity, which determines the presence or absence of astral MTs. While pole morphology was significantly affected, altering nucleation activity surprisingly did not seem to contribute to steady-state spindle length.

Our previous work with katanin identified a differential phosphorylation site present in *X. laevis* katanin and lacking in *X. tropicalis* that reduced MT severing activity (Loughlin et al., 2011). Sequence comparisons of the *X. laevis* and *X. tropicalis* genomes may reveal more examples of differential phosphorylation of mitotic factors. Since phospho-null TPX2 mutants (serine->alanine) of TPX2 at these residues did not alter its MT nucleation activity, regulation may require additional conformational changes or other protein interactions that require further investigation.

These mutants provide the first step in interrogating the contributions of nucleation to spindle architecture. The importance of the c-terminal 7 amino acid sequence requires further study, and perhaps is a crucial site of post-translational regulation, auto-regulation, or an interaction between TPX2 and other proteins. Understanding the mechanistic contribution of TPX2 to nucleation, either directly or indirectly, could provide clues to the positional nucleation within the spindle and resulting architectural effects.

Materials and Methods

Xenopus egg extracts and spindle assembly reactions

X. laevis and *X. tropicalis* egg extracts were prepared and induced to progress through the cell cycle as described (Hannak and Heald, 2006; Maresca and Heald, 2006; Brown *et al.*, 2007). Demembranated *X. laevis* sperm nuclei (to final concentration of 15000 nuclei/µl) were added to CSF extract and released into interphase by the addition of 0.5 mM CaCl2. After approximately 1 hour, nuclei that had decondensed and replicated were flash frozen in extract with 8% glycerol and stored at -80^{o}C. To assemble metaphase spindles, replicated nuclei were resuspended in Egg Lysis Buffer (250 mM sucrose, 50 mM KCl, 2.5 mM MgCl2, 10 mM HEPES pH 7.8) and pelleted by centrifugation at 1600xg for 5 minutes at room temperature. Nuclei were then resuspended in CSF extracts (500 nuclei/µl) and incubated at room temperature for 30-45 minutes while spindle formation occurred. Spindles were visualized by supplementing the extract with X-rhodamine–labeled tubulin (50 µg/ml). For experiments with recombinant protein or inhibitors, all components were added prior to spindle assembly. Where noted, spindle reactions were preserved by fixation with Spindle Fixative (48% glycerol, 1X MMR, 11% formaldehyde, 5 µg/ml Hoechst, (Maresca and Heald, 2006)) under coverglass.

Immunofluorescence analysis

Immunofluorescence staining of fixed spindles was performed according to (Maresca and Heald, 2006). The rabbit antibody to TPX2 raised against 100 N-terminal a.a. was produced by Strategic Diagnostics Inc (SDIX) and used 1:3000. Anti-MBP monoclonal mouse antibody from New England Biolabs (E8030S), was used 1:2000. Spindles in extract were fixed with 3.7% formaldehyde, sedimented through a 40% glycerol cushion onto coverslips, post fixed in 100% methanol and blocked with PBS-1% BSA. Coverslips were incubated with primary antibody, washed extensively with PBS-0.1% NP-40 and incubated with a 1:1000 dilution of secondary antibody (Alexa 488 labeled anti-rabbit or anti-mouse, Invitrogen).

Images were obtained on an Olympus BX51 fluorescence microscope with TRITC, DAPI, and FITC filters (Chroma Technology) and a 40x objective (UPlanFl N, Olympus; NA 0.75) controlled by µManager (http://www.micro-manager. org/) with a Hamamatsu Orca-ER cooled CCD camera. Immunofluorescence analysis was performed as previously described (Loughlin et al., 2011; Wilbur and Heald, 2013). Spindle length was quantified using MATLAB as previously described (Loughlin et al., 2011).

Spinning disk confocal imaging

Confocal slices were taken on a Nikon Spinning Disk confocal microscope (Andor Technologies) with 561nm and 404nm lasers and a 100x objective (Nikon Plan Apo 100x; 1.45 N.A.) controlled by MetaMorph on an Andor iXon3 EMCCD camera.

Protein purification

X. tropicalis and *X. laevis* cDNA for TPX2 were obtained from Open Biosystems and cloned into pMAL-c5x (New England Biolabs) with an additional 6x His tag added c-terminally to the coding sequence (named pMBP-TPX2). Proteins were expressed

overnight at room temperature with 1 mM IPTG and two-step affinity purified first with NiNTA agarose (Sigma) followed by binding to amylose resin (New England Biolabs) in 25 mM HEPES pH 7.7, 250 mM NaCl or KCl, 2 mM MgCl2, and 50 mM sucrose. pMBP-Laevis TPX2 Δ7 was generated by site-directed mutagenesis to remove the amino acids 619-(LSGSIVQ)-625, and pMBP- Laevis TPX2 3SA mutant was changed to alter the proximal serines to alanine 618-ALAGAIVQ-625. pMBP- Trop TPX2 +7 was generated by site-directed mutagenesis to insert the amino acids found in *X. laevis* into the homologous region of the *X. tropicalis* protein: 619T-LSGSIVQ-E620. pMBP-L TPX2 ΔAurA was truncated to remove the n-terminal first 39 amino acids of the protein, and pMBP-L TPX2 ΔEg5 was truncated to remove the last c-terminal 35 amino acids (Bayliss et al., 2003; Eckerdt et al., 2008).

References

Bayliss, R., Sardon, T., Vernos, I., and Conti, E. (2003). Structural basis of Aurora-A activation by TPX2 at the mitotic spindle. Mol Cell *12*, 851–862.

Brown, K. S., Blower, M. D., Maresca, T. J., Grammer, T. C., Harland, R. M., and Heald, R. (2007). Xenopus tropicalis egg extracts provide insight into scaling of the mitotic spindle. J Cell Biol *176*, 765–770.

Eckerdt, F., Eyers, P. A., Lewellyn, A. L., Prigent, C., and Maller, J. L. (2008). Spindle pole regulation by a discrete Eg5-interacting domain in TPX2. Curr Biol *18*, 519–525.

Eckerdt, F., Pascreau, G., Phistry, M., Lewellyn, A. L., DePaoli-Roach, A. A., and Maller, J. L. (2009). Phosphorylation of TPX2 by Plx1 enhances activation of Aurora A. Cell Cycle *8*, 2413–2419.

Eyers, P. A., Erikson, E., Chen, L. G., and Maller, J. L. (2003). A novel mechanism for activation of the protein kinase Aurora A. Curr Biol *13*, 691–697.

Goshima, G. (2011). Identification of a TPX2-like microtubule-associated protein in Drosophila. PLoS ONE *6*, e28120.

Gruss, O. J., Carazo-Salas, R. E., Schatz, C. A., Guarguaglini, G., Kast, J., Wilm, M., Le Bot, N., Vernos, I., Karsenti, E., and Mattaj, I. W. (2001). Ran induces spindle assembly by reversing the inhibitory effect of importin alpha on TPX2 activity. Cell *104*, 83–93.

Guillet, V. *et al.* (2011). Crystal structure of γ-tubulin complex protein GCP4 provides insight into microtubule nucleation. Nat Struct Mol Biol *18*, 915–919.

Hannak, E., and Heald, R. (2006). Investigating mitotic spindle assembly and function in vitro using Xenopus laevis egg extracts. Nat Protoc *1*, 2305–2314.

Hannak, E., Oegema, K., Kirkham, M., Gönczy, P., Habermann, B., and Hyman, A. A. (2002). The kinetically dominant assembly pathway for centrosomal asters in Caenorhabditis elegans is gamma-tubulin dependent. J Cell Biol *157*, 591–602.

Kollman, J. M., Merdes, A., Mourey, L., and Agard, D. A. (2011). Microtubule nucleation by γ-tubulin complexes. Nat Rev Mol Cell Biol *12*, 709–721.

Kollman, J. M., Polka, J. K., Zelter, A., Davis, T. N., and Agard, D. A. (2010). Microtubule nucleating gamma-TuSC assembles structures with 13-fold microtubule-like symmetry. Nature *466*, 879–882.

Loughlin, R., Wilbur, J. D., McNally, F. J., Nédélec, F. J., and Heald, R. (2011). Katanin Contributes to Interspecies Spindle Length Scaling in Xenopus. Cell *147*, 1397–1407.

Maresca, T. J., and Heald, R. (2006). Methods for studying spindle assembly and chromosome condensation in Xenopus egg extracts. Methods Mol. Biol. *322*, 459–474.

Nakajima, H., Toyoshima-Morimoto, F., Taniguchi, E., and Nishida, E. (2003). Identification of a consensus motif for Plk (Polo-like kinase) phosphorylation reveals Myt1 as a Plk1 substrate. J Biol Chem *278*, 25277–25280.

Petry, S., Groen, A. C., Ishihara, K., Mitchison, T. J., and Vale, R. D. (2013). Branching Microtubule Nucleation in Xenopus Egg Extracts Mediated by Augmin and TPX2. Cell *152*, 768–777.

Schatz, C. A., Santarella, R., Hoenger, A., Karsenti, E., Mattaj, I. W., Gruss, O. J., and Carazo-Salas, R. E. (2003). Importin alpha-regulated nucleation of microtubules by TPX2. Embo J *22*, 2060–2070.

Uehara, R., Nozawa, R. S., Tomioka, A., Petry, S., Vale, R. D., Obuse, C., and Goshima, G. (2009). The augmin complex plays a critical role in spindle microtubule generation for mitotic progression and cytokinesis in human cells. Proceedings of the National Academy of Sciences *106*, 6998–7003.

Wilbur, J. D., and Heald, R. (2013). Mitotic spindle scaling during Xenopus development by kif2a and importin α. Elife *2*, e00290.

Chapter 4: Future Study of Spindle Architecture

This dissertation investigates several aspects of spindle morphology that are regulated in part by a MT-associated protein, TPX2. Because a single factor is involved in so many essential processes, including MT density, steady-state spindle length, and pole morphology, this suggests the need for a systems-level investigation toward spindle architecture determination. A more mechanistic understanding of the relationships between TPX2 and its partners, as well as the interplay between the complexes these proteins form, could elucidate how robust spindle structure adapts and is maintained throughout cell division.

Understanding the Role of TPX2 in Microtubule Nucleation

In Chapter 3, we present intriguing results that, for the first time, provide an approach for understanding and modulating MT nucleation. The results, while novel, are just a first step and open up a whole area of investigation that has previously eluded investigators.

The most pressing question is to understand whether the contribution of TPX2 to nucleation is direct or indirect. Based on the complexity of both the MT and the only known nucleator, the γ-tubulin ring complex, it is a reasonable assumption that any other nucleators in the cell would have to be sufficiently large to somehow induce the growth of a structure with 13-fold rotational symmetry. TPX2 alone is unlikely to perform this task, but may work in concert with other factors like γ-TuRC and augmin. Because no canonical tubulin or MT binding domains have been identified in TPX2, direct nucleation seems even less likely. Despite previous experiments showing nucleation of MTs from pure tubulin via TPX2, these data may be compromised by contaminants of MT seeds whose polymerization is stimulated by TPX2 (Schatz *et al.*, 2003). *In vitro* reconstitution studies with higher resolution TIRF microscopy may clarify these ideas.

We identified an important region of the protein, 7 amino acids near the c-terminus, whose function is important in regulating nucleation capacity. Based on prior identification of differential post-translational modification between *X. laevis* and *X. tropicalis* orthologs (Loughlin *et al.*, 2011), we tested whether removal of the serines in this region altered the activity. The results of this were inconclusive, and require further examination. There are many mapped Aurora and Polo phosphorylation sites elsewhere on TPX2 whose function is unknown. Whether or not they interact with this site, or potentially participate with this site in autoregulation, would be an intriguing line of inquiry.

The structure of TPX2 is difficult to predict computationally from the primary sequence, and the peptides that have been crystallized are unstructured domains (Bayliss *et al.*, 2003). Taken with the observational evidence of the aggregation of recombinant TPX2 and stability of GST-TPX2 dimers, it is a reasonable hypothesis that TPX2 exists as only an oligomer or in complex with other proteins in the cell. It is possible the 7 amino acid region we identified is important for oligomerization or for binding other proteins to stabilize TPX2 in the cell. The discovery of these species orthologs with different

activities can allow for the immediate study of complex formation by gel filtration and other methods. Ultimately, the structure of this protein is the most important key to understanding the function and interactions of TPX2, and that should be the primary goal of future study.

Identifying Contributions of Positional Nucleation to Spindle Architecture

With the TPX2 mutants described in both Chapters 2 and 3, we now have tools to interrogate the role of nucleation in spindle architecture. Our results indicate that endogenous TPX2 nucleation contributes primarily to spindle pole architecture, possibly because TPX2 activity is primarily targeted to pole by interaction with dynein. If the *X. laevis* and *X. tropicalis* TPX2 orthologs could be modified with targeting domains to different regions of the spindle, that could more precisely test the contribution of location of MT nucleation in steady-state spindle morphology. Additionally, depending on the characteristics of TPX2 learned through the previous aim, further exploitation of the mechanisms of its functions could be used to answer questions about other features of spindle structure.

Characterizing the TPX2 and Eg5 Interaction

This work clearly indicates an important role for the TPX2-Eg5 interaction in mediating spindle length. While only one parameter that describes spindle architecture, length is a crucial factor to ensure that chromosomes are separated by enough distance to be properly transmitted to daughter cells.

Here we show that TPX2 requires the Eg5 interaction to properly localize to the spindle, while another work conversely shows that TPX2 is required for Eg5 localization (Ma *et al.*, 2011; Gable *et al.*, 2012). Despite intrinsic MT interaction by both proteins, it is possible that complex formation between Eg5 and TPX2 is required for both to function in spindle assembly and maintenance. To clarify these events, it is essential to map the interaction domain on the Eg5 protein and determine how the structure of the TPX2-Eg5 complex interacts with MTs. While TPX2 has been shown to halt Eg5 motor activity in purified systems, it is unclear if this is promoted by tethering to MTs or by TPX2 binding to Eg5 alone. Furthermore, since targeting of both of these proteins to the pole is thought to be mediated by dynein, which has a functional consequence on the activity of these proteins by polar localization, it is paramount to understand how this motor is involved in complex activity in the spindle.

These structural studies will also serve to confirm the model of interaction and spindle regulation posited by the experimental results in this dissertation.

Toward a Comprehensive View of Spindle Architecture

The metaphase spindle is an incredibly dynamic structure, with the turnover of MTs, and therefore the bound proteins, on the order of seconds. What is less appreciated is how the steady-state structure is maintained dynamically. This also supports the belief that spindles are adaptable structures that can modulate architectural characteristics over the time of cell division, and potentially in the face of perturbation.

The spindles described here contain metazoan-specific characteristics of size and MT organization. There is great variation of spindle architecture throughout evolution, spanning from tens of MTs to hundreds of thousands, one MT per kinetochore to dozens, and single microns to tens in length. Furthermore, MTs vary greatly in their distribution between populations of astral, spindle, or kinetochore MTs. Currently we do not have a fundamental understanding of how this is determined.

TPX2 is an interesting candidate for contributing to some of these evolutionary differences. As discussed in Chapter 2, the characterized domains of TPX2 are not well-conserved among species, and therefore the TPX2 orthologs found in each species would have functionality based on the present domains. We can speculate that this is an evolutionary tool to tune spindle architecture by selecting the activities necessary to promote robust spindle structure in each species. Because hundreds of factors are involved in spindle assembly, we may find other examples of this motif bioinformatically.

With advances in understanding MT nucleation that spur from this study, as well as technical progress in super-resolution and electron microscopy, we will be able to improve existing computational models to integrate the available data and present a more clear picture of spindle architecture and morphology.

References

Bayliss, R., Sardon, T., Vernos, I., and Conti, E. (2003). Structural basis of Aurora-A activation by TPX2 at the mitotic spindle. Mol Cell *12*, 851–862.

Gable, A. *et al.* (2012). Dynamic reorganization of Eg5 in the mammalian spindle throughout mitosis requires dynein and TPX2. Mol. Biol. Cell *23*, 1254–1266.

Loughlin, R., Wilbur, J. D., McNally, F. J., Nédélec, F. J., and Heald, R. (2011). Katanin Contributes to Interspecies Spindle Length Scaling in Xenopus. Cell *147*, 1397–1407.

Ma, N., Titus, J., Gable, A., Ross, J. L., and Wadsworth, P. (2011). TPX2 regulates the localization and activity of Eg5 in the mammalian mitotic spindle. J Cell Biol *195*, 87–98.

Schatz, C. A., Santarella, R., Hoenger, A., Karsenti, E., Mattaj, I. W., Gruss, O. J., and Carazo-Salas, R. E. (2003). Importin alpha-regulated nucleation of microtubules by TPX2. Embo J *22*, 2060–2070.

REFERENCES

Ban, K. H., Torres, J. Z., Miller, J. J., Mikhailov, A., Nachury, M. V., Tung, J. J., Rieder, C. L., and Jackson, P. K. (2007). The END network couples spindle pole assembly to inhibition of the anaphase-promoting complex/cyclosome in early mitosis. Dev. Cell *13*, 29–42.

Bayliss, R., Sardon, T., Vernos, I., and Conti, E. (2003). Structural basis of Aurora-A activation by TPX2 at the mitotic spindle. Mol Cell *12*, 851–862.

Bird, A. W., and Hyman, A. A. (2008). Building a spindle of the correct length in human cells requires the interaction between TPX2 and Aurora A. J Cell Biol *182*, 289–300.

Brown, K. S., Blower, M. D., Maresca, T. J., Grammer, T. C., Harland, R. M., and Heald, R. (2007). Xenopus tropicalis egg extracts provide insight into scaling of the mitotic spindle. J Cell Biol *176*, 765–770.

Brugués, J., Nuzzo, V., Mazur, E., and Needleman, D. J. (2012). Nucleation and transport organize microtubules in metaphase spindles. Cell *149*, 554–564.

Brunet, S., Sardon, T., Zimmerman, T., Wittmann, T., Pepperkok, R., Karsenti, E., and Vernos, I. (2004). Characterization of the TPX2 Domains Involved in Microtubule Nucleation and Spindle Assembly in Xenopus Egg Extracts. Mol. Biol. Cell *15*, 5318–5328.

Cameron, L. A., Yang, G., Cimini, D., Canman, J. C., Kisurina-Evgenieva, O., Khodjakov, A., Danuser, G., and Salmon, E. D. (2006). Kinesin 5-independent poleward flux of kinetochore microtubules in PtK1 cells. J Cell Biol *173*, 173–179.

Carazo-Salas, R. E., Guarguaglini, G., Gruss, O. J., Segref, A., Karsenti, E., and Mattaj, I. W. (1999). Generation of GTP-bound Ran by RCC1 is required for chromatin-induced mitotic spindle formation. Nature *400*, 178–181.

Chi, N. C., Adam, E. J., and Adam, S. A. (1997). Different binding domains for Ran-GTP and Ran-GDP/RanBP1 on nuclear import factor p97. J Biol Chem *272*, 6818–6822.

Chrétien, D., Metoz, F., Verde, F., Karsenti, E., and Wade, R. H. (1992). Lattice defects in microtubules: protofilament numbers vary within individual microtubules. J Cell Biol *117*, 1031–1040.

Cole, D. G., Saxton, W. M., Sheehan, K. B., and Scholey, J. M. (1994). A “slow” homotetrameric kinesin-related motor protein purified from Drosophila embryos. J Biol Chem *269*, 22913–22916.

Colombié, N., Cullen, C. F., Brittle, A. L., Jang, J. K., Earnshaw, W. C., Carmena, M., McKim, K., and Ohkura, H. (2008). Dual roles of Incenp crucial to the assembly of the acentrosomal metaphase spindle in female meiosis. Development *135*, 3239–3246.

Compton, D. A. (1998). Focusing on spindle poles. J Cell Sci *111 (Pt 11)*, 1477–1481.

Crane, R., Gadea, B., Littlepage, L., Wu, H., and Ruderman, J. V. (2012). Aurora A, Meiosis and Mitosis. Biology of the Cell *96*, 215–229.

Downing, K. H., and Nogales, E. (1998). Tubulin and microtubule structure. Curr Opin Cell Biol *10*, 16–22.

Eckerdt, F., Eyers, P. A., Lewellyn, A. L., Prigent, C., and Maller, J. L. (2008). Spindle pole regulation by a discrete Eg5-interacting domain in TPX2. Curr Biol *18*, 519–525.

Eckerdt, F., Pascreau, G., Phistry, M., Lewellyn, A. L., DePaoli-Roach, A. A., and Maller, J. L. (2009). Phosphorylation of TPX2 by Plx1 enhances activation of Aurora A. Cell Cycle *8*, 2413–2419.

Endow, S. A., Chandra, R., Komma, D. J., Yamamoto, A. H., and Salmon, E. D. (1994). Mutants of the Drosophila ncd microtubule motor protein cause centrosomal and spindle pole defects in mitosis. J Cell Sci *107 (Pt 4)*, 859–867.

Eyers, P. A., Erikson, E., Chen, L. G., and Maller, J. L. (2003). A novel mechanism for activation of the protein kinase Aurora A. Curr Biol *13*, 691–697.

Fitzharris, G. (2009). A shift from kinesin 5-dependent metaphase spindle function during preimplantation development in mouse. Development *136*, 2111–2119.

Gable, A. *et al.* (2012). Dynamic reorganization of Eg5 in the mammalian spindle throughout mitosis requires dynein and TPX2. Mol. Biol. Cell *23*, 1254–1266.

Gadea, B. B., and Ruderman, J. V. (2005). Aurora kinase inhibitor ZM447439 blocks chromosome-induced spindle assembly, the completion of chromosome condensation, and the establishment of the spindle integrity checkpoint in Xenopus egg extracts. Mol. Biol. Cell *16*, 1305–1318.

Gadea, B. B., and Ruderman, J. V. (2006). Aurora B is required for mitotic chromatin-induced phosphorylation of Op18/Stathmin. Proc Natl Acad Sci USA *103*, 4493–4498.

Giesecke, A., and Stewart, M. (2010). Novel Binding of the Mitotic Regulator TPX2 (Target Protein for Xenopus Kinesin-like Protein 2) to Importin. Journal of Biological Chemistry *285*, 17628–17635.

Goshima, G. (2011). Identification of a TPX2-like microtubule-associated protein in Drosophila. PLoS ONE *6*, e28120.

Goshima, G., Mayer, M., Zhang, N., Stuurman, N., and Vale, R. D. (2008). Augmin: a protein complex required for centrosome-independent microtubule generation within the spindle. J Cell Biol *181*, 421–429.

Goshima, G., Wollman, R., Goodwin, S. S., Zhang, N., Scholey, J. M., Vale, R. D., and

Stuurman, N. (2007). Genes required for mitotic spindle assembly in Drosophila S2 cells. Science *316*, 417–421.

Goshima, G., Wollman, R., Stuurman, N., Scholey, J. M., and Vale, R. D. (2005). Length control of the metaphase spindle. Curr Biol *15*, 1979–1988.

Greenan, G., Brangwynne, C. P., Jaensch, S., Gharakhani, J., Jülicher, F., and Hyman, A. A. (2010). Centrosome size sets mitotic spindle length in Caenorhabditis elegans embryos. Curr Biol *20*, 353–358.

Gruss, O. J., Carazo-Salas, R. E., Schatz, C. A., Guarguaglini, G., Kast, J., Wilm, M., Le Bot, N., Vernos, I., Karsenti, E., and Mattaj, I. W. (2001). Ran induces spindle assembly by reversing the inhibitory effect of importin alpha on TPX2 activity. Cell *104*, 83–93.

Guillet, V. *et al.* (2011). Crystal structure of γ-tubulin complex protein GCP4 provides insight into microtubule nucleation. Nat Struct Mol Biol *18*, 915–919.

Halpin, D., Kalab, P., Wang, J., Weis, K., and Heald, R. (2011). Mitotic spindle assembly around RCC1-coated beads in Xenopus egg extracts. PLoS Biol *9*, e1001225.

Hannak, E., and Heald, R. (2006). Investigating mitotic spindle assembly and function in vitro using Xenopus laevis egg extracts. Nat Protoc *1*, 2305–2314.

Hannak, E., Oegema, K., Kirkham, M., Gönczy, P., Habermann, B., and Hyman, A. A. (2002). The kinetically dominant assembly pathway for centrosomal asters in Caenorhabditis elegans is gamma-tubulin dependent. J Cell Biol *157*, 591–602.

Heald, R., Tournebize, R., Blank, T., Sandaltzopoulos, R., Becker, P., Hyman, A., and Karsenti, E. (1996). Self-organization of microtubules into bipolar spindles around artificial chromosomes in Xenopus egg extracts. Nature *382*, 420–425.

Helmke, K. J., Heald, R., and Wilbur, J. D. (2013). Interplay between spindle architecture and function. Int Rev Cell Mol Biol *306*, 83–125.

Holy, T. E., and Leibler, S. (1994). Dynamic instability of microtubules as an efficient way to search in space. Proc Natl Acad Sci USA *91*, 5682–5685.

Jensen, C. G. (1982). Dynamics of spindle microtubule organization: kinetochore fiber microtubules of plant endosperm. J Cell Biol *92*, 540–558.

Kalab, P., Pralle, A., Isacoff, E. Y., Heald, R., and Weis, K. (2006). Analysis of a RanGTP-regulated gradient in mitotic somatic cells. Nat Cell Biol *440*, 697–701.

Kalab, P., Pu, R. T., and Dasso, M. (1999). The ran GTPase regulates mitotic spindle assembly. Curr Biol *9*, 481–484.

Kalab, P., Weis, K., and Heald, R. (2002). Visualization of a Ran-GTP Gradient in

Interphase and Mitotic Xenopus Egg Extracts. Science *295*, 2452–2456.

Kapoor, T. M., Mayer, T. U., Coughlin, M. L., and Mitchison, T. J. (2000). Probing spindle assembly mechanisms with monastrol, a small molecule inhibitor of the mitotic kinesin, Eg5. J Cell Biol *150*, 975–988.

Karsenti, E. (2005). TPX or Not TPX? Mol Cell *19*, 431–432.

Khodjakov, A. (2003). Minus-end capture of preformed kinetochore fibers contributes to spindle morphogenesis. J Cell Biol *160*, 671–683.

Khodjakov, A., Cole, R. W., Oakley, B. R., and Rieder, C. L. (2000). Centrosome-independent mitotic spindle formation in vertebrates. Curr Biol *10*, 59–67.

Kollman, J. M., Merdes, A., Mourey, L., and Agard, D. A. (2011). Microtubule nucleation by γ-tubulin complexes. Nat Rev Mol Cell Biol *12*, 709–721.

Kollman, J. M., Polka, J. K., Zelter, A., Davis, T. N., and Agard, D. A. (2010). Microtubule nucleating gamma-TuSC assembles structures with 13-fold microtubule-like symmetry. Nature *466*, 879–882.

Kollu, S., Bakhoum, S. F., and Compton, D. A. (2009). Interplay of microtubule dynamics and sliding during bipolar spindle formation in mammalian cells. Curr Biol *19*, 2108–2113.

Kraft, C., Herzog, F., Gieffers, C., Mechtler, K., Hagting, A., Pines, J., and Peters, J.-M. (2003). Mitotic regulation of the human anaphase-promoting complex by phosphorylation. Embo J *22*, 6598–6609.

Kufer, T. A., Silljé, H. H. W., Körner, R., Gruss, O. J., meraldi, P., and Nigg, E. A. (2002). Human TPX2 is required for targeting Aurora-A kinase to the spindle. J Cell Biol *158*, 617–623.

Levy, D. L., and Heald, R. (2010). Nuclear Size Is Regulated by Importin α and Ntf2 in Xenopus. Cell *143*, 288–298.

Loughlin, R., Heald, R., and Nédélec, F. (2010). A computational model predicts Xenopus meiotic spindle organization. J Cell Biol *191*, 1239–1249.

Loughlin, R., Wilbur, J. D., McNally, F. J., Nédélec, F. J., and Heald, R. (2011). Katanin Contributes to Interspecies Spindle Length Scaling in Xenopus. Cell *147*, 1397–1407.

Ma, N., Titus, J., Gable, A., Ross, J. L., and Wadsworth, P. (2011). TPX2 regulates the localization and activity of Eg5 in the mammalian mitotic spindle. J Cell Biol *195*, 87–98.

Ma, N., Tulu, U. S., Ferenz, N. P., Fagerstrom, C., Wilde, A., and Wadsworth, P. (2010). Poleward transport of TPX2 in the mammalian mitotic spindle requires dynein, Eg5, and microtubule flux. Mol. Biol. Cell *21*, 979–988.

Mahoney, N. M., Goshima, G., Douglass, A. D., and Vale, R. D. (2006). Making Microtubules and Mitotic Spindles in Cells without Functional Centrosomes. Current Biology *16*, 564–569.

Maiato, H., Rieder, C. L., and Khodjakov, A. (2004). Kinetochore-driven formation of kinetochore fibers contributes to spindle assembly during animal mitosis. J Cell Biol *167*, 831–840.

Maliga, Z., and Mitchison, T. J. (2006). Small-molecule and mutational analysis of allosteric Eg5 inhibition by monastrol. BMC Chem Biol *6*, 2.

Maresca, T. J., and Heald, R. (2006). Methods for studying spindle assembly and chromosome condensation in Xenopus egg extracts. Methods Mol. Biol. *322*, 459–474.

Merdes, A., Heald, R., Samejima, K., Earnshaw, W. C., and Cleveland, D. W. (2000). Formation of spindle poles by dynein/dynactin-dependent transport of NuMA. J Cell Biol *149*, 851–862.

Mitchison, T. J., and Kirschner, M. W. (1985). Properties of the kinetochore in vitro. I. Microtubule nucleation and tubulin binding. J Cell Biol *101*, 755–765.

Mitchison, T., and Kirschner, M. (1984a). Dynamic instability of microtubule growth. Nature *312*, 237–242.

Mitchison, T., and Kirschner, M. (1984b). Microtubule assembly nucleated by isolated centrosomes. Nature *312*, 232–237.

Miyamoto, D. T., Perlman, Z. E., Burbank, K. S., Groen, A. C., and Mitchison, T. J. (2004). The kinesin Eg5 drives poleward microtubule flux in Xenopus laevis egg extract spindles. J Cell Biol *167*, 813–818.

Nachury, M. V., Maresca, T. J., Salmon, W. C., Waterman-Storer, C. M., Heald, R., and Weis, K. (2001). Importin beta is a mitotic target of the small GTPase Ran in spindle assembly. Cell *104*, 95–106.

Needleman, D. J., Groen, A., Ohi, R., Maresca, T., Mirny, L., and Mitchison, T. (2010). Fast microtubule dynamics in meiotic spindles measured by single molecule imaging: evidence that the spindle environment does not stabilize microtubules. Mol. Biol. Cell *21*, 323–333.

Ohba, T., Nakamura, M., Nishitani, H., and Nishimoto, T. (1999). Self-organization of microtubule asters induced in Xenopus egg extracts by GTP-bound Ran. Science *284*, 1356–1358.

Ohi, R., Sapra, T., Howard, J., and Mitchison, T. J. (2004). Differentiation of cytoplasmic and meiotic spindle assembly MCAK functions by Aurora B-dependent phosphorylation. Mol. Biol. Cell *15*, 2895–2906.

Paul, R., Wollman, R., Silkworth, W. T., Nardi, I. K., Cimini, D., and Mogilner, A. (2009). Computer simulations predict that chromosome movements and rotations accelerate mitotic spindle assembly without compromising accuracy. Proc Natl Acad Sci USA *106*, 15708–15713.

Pepper, D. A., and Brinkley, B. R. (1979). Microtubule initiation at kinetochores and centrosomes in lysed mitotic cells. Inhibition of site-specific nucleation by tubulin antibody. J Cell Biol *82*, 585–591.

Petry, S., Groen, A. C., Ishihara, K., Mitchison, T. J., and Vale, R. D. (2013). Branching Microtubule Nucleation in Xenopus Egg Extracts Mediated by Augmin and TPX2. Cell *152*, 768–777.

Petry, S., Pugieux, C., Nedelec, F. J., and Vale, R. D. (2011). Augmin promotes meiotic spindle formation and bipolarity in Xenopus egg extracts. Proceedings of the National Academy of Sciences *108*, 14473–14478.

Rieder, C. L. (2005). Kinetochore fiber formation in animal somatic cells: dueling mechanisms come to a draw. Chromosoma *114*, 310–318.

Ruchaud, S., Carmena, M., and Earnshaw, W. C. (2007). Chromosomal passengers: conducting cell division. Nat Rev Mol Cell Biol *8*, 798–812.

Sampath, S. C., Ohi, R., Leismann, O., Salic, A., Pozniakovski, A., and Funabiki, H. (2004). The Chromosomal Passenger Complex Is Required for Chromatin-Induced Microtubule Stabilization and Spindle Assembly. Cell *118*, 187–202.

Sawin, K. E., LeGuellec, K., Philippe, M., and Mitchison, T. J. (1992). Mitotic spindle organization by a plus-end-directed microtubule motor. Nature *359*, 540–543.

Schatz, C. A., Santarella, R., Hoenger, A., Karsenti, E., Mattaj, I. W., Gruss, O. J., and Carazo-Salas, R. E. (2003). Importin alpha-regulated nucleation of microtubules by TPX2. Embo J *22*, 2060–2070.

Somma, M. P. *et al.* (2008). Identification of Drosophila mitotic genes by combining co-expression analysis and RNA interference. PLoS Genet *4*, e1000126.

Song, L., and Rape, M. (2010). Regulated degradation of spindle assembly factors by the anaphase-promoting complex. Mol Cell *38*, 369–382.

Tirnauer, J. S., Salmon, E. D., and Mitchison, T. J. (2004). Microtubule plus-end dynamics in Xenopus egg extract spindles. Mol. Biol. Cell *15*, 1776–1784.

Torosantucci, L., De Luca, M., Guarguaglini, G., Lavia, P., and Degrassi, F. (2008). Localized RanGTP accumulation promotes microtubule nucleation at kinetochores in somatic mammalian cells. Mol. Biol. Cell *19*, 1873–1882.

Tsai, M.-Y., Wiese, C., Cao, K., Martin, O., Donovan, P., Ruderman, J., Prigent, C., and

Zheng, Y. (2003). A Ran signalling pathway mediated by the mitotic kinase Aurora A in spindle assembly. Nat Cell Biol *5*, 242–248.

Tugendreich, S., Tomkiel, J., Earnshaw, W., and Hieter, P. (1995). CDC27Hs colocalizes with CDC16Hs to the centrosome and mitotic spindle and is essential for the metaphase to anaphase transition. Cell *81*, 261–268.

Tulu, U. S., Fagerstrom, C., Ferenz, N. P., and Wadsworth, P. (2006). Molecular requirements for kinetochore-associated microtubule formation in mammalian cells. Curr Biol *16*, 536–541.

Uehara, R., Nozawa, R. S., Tomioka, A., Petry, S., Vale, R. D., Obuse, C., and Goshima, G. (2009). The augmin complex plays a critical role in spindle microtubule generation for mitotic progression and cytokinesis in human cells. Proceedings of the National Academy of Sciences *106*, 6998–7003.

Uteng, M., Hentrich, C., Miura, K., Bieling, P., and Surrey, T. (2008). Poleward transport of Eg5 by dynein-dynactin in Xenopus laevis egg extract spindles. J Cell Biol *182*, 715–726.

van den Wildenberg, S. M. J. L., Tao, L., Kapitein, L. C., Schmidt, C. F., Scholey, J. M., and Peterman, E. J. G. (2008). The homotetrameric kinesin-5 KLP61F preferentially crosslinks microtubules into antiparallel orientations. Curr Biol *18*, 1860–1864.

Vanneste, D., Takagi, M., Imamoto, N., and Vernos, I. (2009). The Role of Hklp2 in the Stabilization and Maintenance of Spindle Bipolarity. Current Biology *19*, 1712–1717.

Walczak, C. E., and Heald, R. (2008). Mechanisms of Mitotic Spindle Assembly and Function. In: International Review of Cytology, Elsevier, 111–158.

Walczak, C. E., Vernos, I., Mitchison, T. J., Karsenti, E., and Heald, R. (1998). A model for the proposed roles of different microtubule-based motor proteins in establishing spindle bipolarity. Curr Biol *8*, 903–913.

Weis, K., Dingwall, C., and Lamond, A. I. (1996). Characterization of the nuclear protein import mechanism using Ran mutants with altered nucleotide binding specificities. Embo J *15*, 7120–7128.

Wilbur, J. D., and Heald, R. (2013). Mitotic spindle scaling during Xenopus development by kif2a and importin α. Elife *2*, e00290.

Wilde, A., and Zheng, Y. (1999). Stimulation of microtubule aster formation and spindle assembly by the small GTPase Ran. Science *284*, 1359–1362.

Williamson, A., Wickliffe, K. E., Mellone, B. G., Song, L., Karpen, G. H., and Rape, M. (2009). Identification of a physiological E2 module for the human anaphase-promoting complex. Proceedings of the National Academy of Sciences *106*, 18213–18218.

Wittmann, T., Boleti, H., Antony, C., Karsenti, E., and Vernos, I. (1998). Localization of the kinesin-like protein Xklp2 to spindle poles requires a leucine zipper, a microtubule-associated protein, and dynein. J Cell Biol *143*, 673–685.

Wittmann, T., Wilm, M., Karsenti, E., and Vernos, I. (2000). TPX2, A novel xenopus MAP involved in spindle pole organization. J Cell Biol *149*, 1405–1418.

Wollman, R., Cytrynbaum, E. N., Jones, J. T., and Meyer, T. (2005). Efficient chromosome capture requires a bias in the “search-and-capture”process during mitotic-spindle assembly. Current Biology.

Wu, J. Q., and Kornbluth, S. (2008). Across the meiotic divide - CSF activity in the post-Emi2/XErp1 era. J Cell Sci *121*, 3509–3514.

Yang, G., Cameron, L. A., Maddox, P. S., Salmon, E. D., and Danuser, G. (2008). Regional variation of microtubule flux reveals microtubule organization in the metaphase meiotic spindle. J Cell Biol *182*, 631–639.

Zhang, C., Hughes, M., and Clarke, P. R. (1999). Ran-GTP stabilises microtubule asters and inhibits nuclear assembly in Xenopus egg extracts. J Cell Sci *112 (Pt 14)*, 2453–2461.